SYNTHESIS AND CHARACTERIZATION OF NANOIZED SCALE INHIBITOR

FOR INCREASED TREATMENT LIFETIME

A Thesis

by

JOSHUA JOEL HERNANDEZ

Submitted to the Office of Graduate and Professional Studies of
Texas A&M University
in partial fulfillment of the requirements for the degree of

MASTER OF SCIENCE

Chair of Committee,   Jenn-Tai Liang
Co-Chair of Committee,   Huili Guan
Committee Member,   Karen L. Wooley

Head of Department,   A. Daniel Hill

August 2017

Major Subject: Petroleum Engineering

ABSTRACT

Scale formation is an ongoing production issue in the oil and gas industry where inorganic salts can form deposits downhole or in production facilities. These deposits can severely hinder production and lead to significant lost revenue and remediation costs. Scale inhibitors are compounds which prevent the production of insoluble deposits, and their efficacy can be measured by their brine compatibility, minimum inhibition concentration (MIC), and retention in rock. This project details the development of a novel cross-linked scale inhibitor (i.e. nanoized scale inhibitor or NSI) with the following characteristics: high brine compatibility, effective release profile, and high retention in porous media. Experimental analysis of polymeric nanoized scale inhibitor (NSI) yielded effective release of durations up to 40 days, a low MIC of ~3 ppm under static conditions, and 15-55% retention of NSI in quartz sandpack experiments after 6 PV of brine throughput. The NSI retention results proved to be much higher than the linear polymer scale inhibitor retention of ~3% after 6 PV of throughput. Initial retention values showed to be highly dependent on the concentration of SI injected into the sandpack, and retention versus throughput proved to be largely dependent on particle size. QCM-D experiments were performed on the NSI and linear scale inhibitor samples to investigate adsorption via electrostatic particle interactions. Experimental results suggested that the NSI system interacts primarily with positive surface charge, and further suggested that retention in a quartz sandpack is largely due to mechanical lodging of NSI in pore space.

ACKNOWLEDGEMENTS

I would like to thank my committee chair, Jenn-Tai Liang, and my committee members, Huili Guan, and Karen Wooley, for their critique, guidance, and support throughout the course of this research.

I give sincere a thank you to Texas A&M University and the Office of Graduate Studies, for making my education and research possible. It has truly been a pleasure.

I would also like to thank all those who contributed to the data collection for this research. Corbin Andersen, EbunOluwa Andrew, Dinara Dussenova, Huili Guan, Austin Lim, Ying-Ying Lin, and Shawn Sun all contributed greatly to the completion of the project.

CONTRIBUTORS AND FUNDING SOURCES

NOMENCLATURE

[ ]	Concentration
$BaSO_4$	Barium Sulfate
$CaCO_3$	Calcium Carbonate
CAPEX	Capital Expenditure
C_{1f}	Final inhibitor concentration (mg/L)
C_m	Mobile-phase inhibitor concentration
C_o	Initial inhibitor concentration (mg/L)
DETPMP	Diethylenetriamine penta (methylene phosphonic acid)
DI	Deionized Water
DLS	Dynamic Light Scattering
DTPA	Diethylene-Triamine-Penta Acetic acid
EDAX	Energy-dispersive X-ray Spectroscopy
EDTA	Ethylenediamine tetraacetic acid
ESEM	Environmental Scanning Electron Microscopy/Microscope
EPM	Electron Probe Microscope
ESI	Encapsulated Scale Inhibitor
FAST	Flow Assurance and Scale Team
FW	Formation Water
HEDP	Hexamethylenediamine tetramethylene phosphonic acid
ICP	Inductively Coupled Plasma
IE	Inhibition Efficiency

Ksp	Solubility Product
L	Liter
m/V	Mass Volume Ratio
mg/L	Milligrams per Liter
MIC	Minimum Inhibitor Concentration
MW	Molecular Weight
NaOH	Sodium Hydroxide
NDIR	Nondispersive Infrared
nm	Nanometer
NPT	National Pipe Thread
NSI	Nanoized Scale Inhibitor
OMTHP	Octa-methylene-tetramine hexa (methylene-phosphonic acid)
OPEX	Operating Expenses
P	Pressure
PEI	polyethylenimine
pH	Negative logarithm of the solution hydrogen ion activity
ppm	Parts Per Million
PTFE	Polytetrafluoroethylene
PV	Pore Volume
QCM-D	Quartz Crystal Microbalance with Dissipation Monitoring
SEM	Scanning Electron Microscopy
SI	Scale Inhibitor

SR	Saturation Ratio
SW	Sea Water
T	Temperature
TDS	Total dissolved solids
t	Time
XRD	X-Ray Diffraction
α, β	Freundlich Constants
$\Gamma(C)$	Rock adsorption isotherm, where C = concentration of inhibitor
Γapp	Apparent adsorption
ρ	Density
Φ	Fraction of the Precipitation
ϕ	Porosity

TABLE OF CONTENTS

LIST OF FIGURES

LIST OF TABLES

1. BACKGROUND

1.1 Introduction

Despite the recent push from many nations to develop alternative and renewable sources of energy, oil and gas will continue to be the major contributor to the immediate needs of global energy for years. Within the latter half of the 20th century, increasing demands of oil and gas consumption and the depletion of conventional reserves pushed the production into increasingly difficult frontiers such as offshore deep or ultra-deep water operations or onshore unconventional oil and gas. The U.S. Gulf of Mexico (GOM) crude oil production is estimated to increase to record high levels in 2017, even as oil prices remain low (Figure 1). According to the Energy Information Administration (EIA) Gulf of Mexico production is expected to account for 18% and 21% of total forecast U.S. crude oil production in 2016 and 2017, respectively. Additionally, U.S. tight oil and shale gas production is only predicted to increase in the foreseeable future (Figure 2). Tight oil contributed to 52% of total U.S. crude production in 2015, and similarly shale gas contributed to 50% of total U.S. natural gas production (Murali & Aloulou, 2016). It is evident that these trends will continue into the foreseeable future.
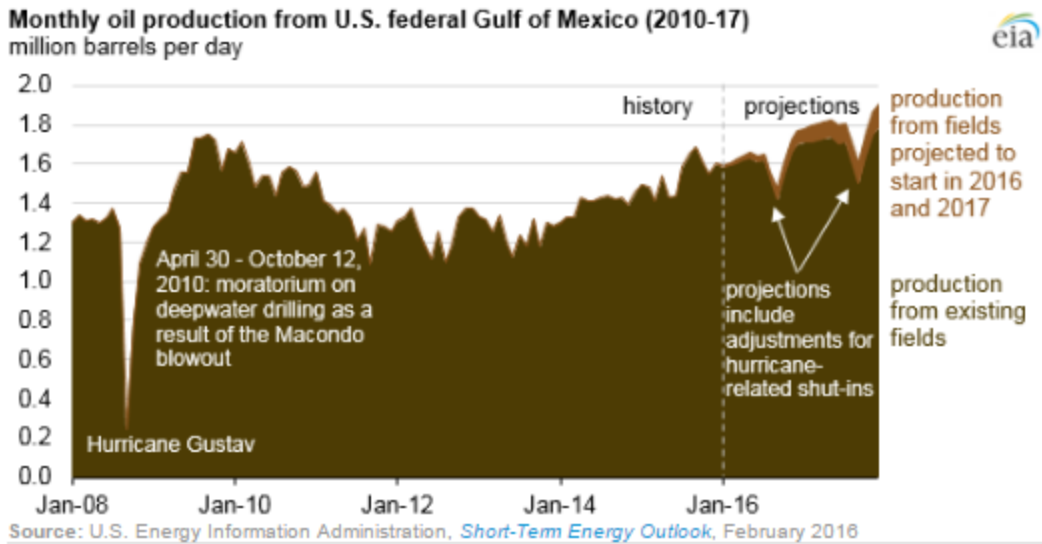
Figure 1: Monthly Oil Production from U.S. Federal Gulf of Mexico (Yen, 2016)
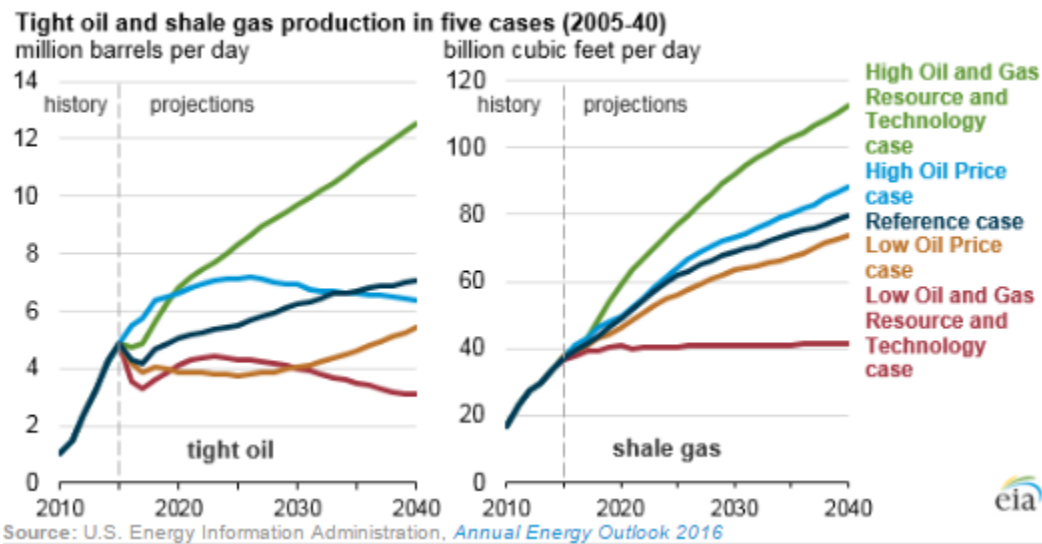
Figure 2: Tight and Shale Gas Production Predictions (Murali & Aloulou, 2016)

The advent of new technologies in drilling or pumping systems made production from deep and tight formations possible. However, production from these sources can have significant corrosion, hydrate formation, and scale control issues in flow assurance. These issues can be exacerbated by conditions in deep water reservoirs, which are typically characterized by high temperatures (>150 °C), pressures (>14,000 psi) and high total dissolved solids (TDS) values (>300,000 mg/L). The presence of high salt or mineral concentrations as well as the drop in temperature and pressure as production fluids leave the reservoir can cause significant scale problems in both wellbore and surface equipment. Scale (Figure 3 and Figure 4) is the precipitate that forms on surfaces in contact with production fluids, and these deposits can extremely insoluble. Scaling typically forms when the equilibrium of the fluids in the formation is disturbed or when two incompatible brines mix (Frenier & Ziauddin, 2008). Table 1 contains a list of the common scales that occur in the oil and gas production.
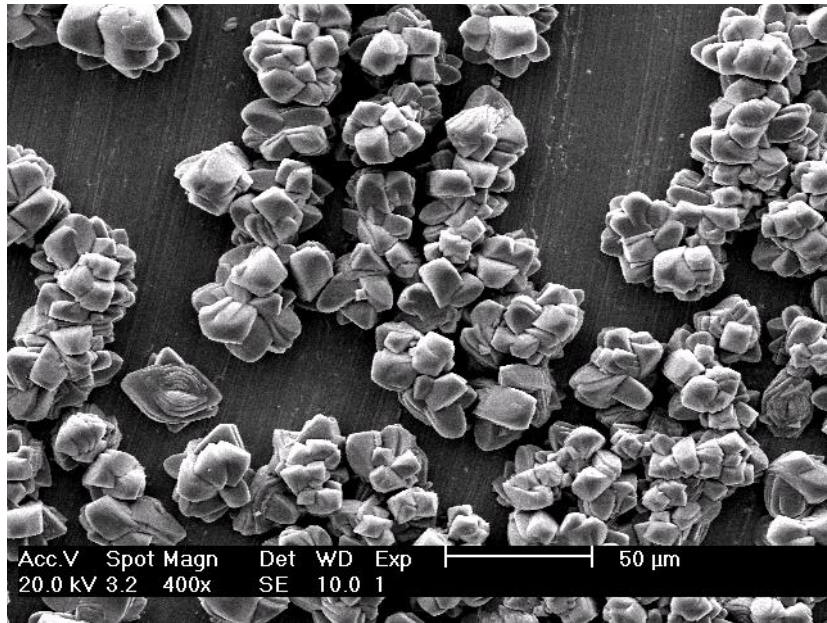
Figure 3: EM Image of Crystalline Scale Deposits (Mackey, 2007)

Figure 4: Typical Oilfield Scales (Mackey, 2007) – (Left & Center) Scale and other debris formation along sides of pipe. (Right) Suspended particles in plug formation and filtration equipment.

Oilfield scales typically consist of one or more types of inorganic deposit along with other debris such as organic precipitates, sand, and corrosion products (Figure 4).

4

Scale deposits can cause formation damage near the wellbore, create blockages in perforations or gravel packs, restrict or block flow lines, lead to valve and choke failure, increase pump wear, cause corrosion underneath deposits, and can potentially be radioactive. Scale deposits can also lead to suspended particles in plugs and filtration equipment, and can reduce the oil/water separator efficiency (Mackey, 2007).

Table 1: Common Scale in Oil and Gas Production

Molecular Formula	Source of Cation	Source of Anion	Main Crystal
$CaCO_3$	Formation Brine	Formation Water	Calcite
$BaSO_4$	Formation Brine	Sea Water	Barite
$CaSO_4-nH_2O$	Formation Brine	Sea Water	Anhydrite, gypsum
$SrSO_4$	Formation Brine	Sea Water	Celestite
$FeCO3$	Corrosion	Formation Brine	Siderite
$Fe(OH)_2$, Fe_2O_3, Fe_3O_4	Corrosion	Thermal and Oxygen-Rich Injection Water	Magnetite, Hematite
FeS, FeS_2	Corrosion	Sulfate-Reducing Bacteria	Pyrite

The most troublesome of the common scales seen in Table 1 include the barium and strontium compounds, as they are extremely insoluble in water and have limited solubility in acid. Therefore, prevention is the primary means of dealing with scale formation and includes the application of scale inhibitors to help maintain the integrity

of equipment during drilling and completion as well as throughout the lifetime of production of a well.

Chemical treatment is typically used to reduce the concentration of scale-forming compounds that can accumulate in production wells, water and disposal wells, flowlines, and surface equipment. The most common treatment involves the use of water soluble chemical scale inhibitors, which are injected (or "squeezed") into the formation rock via production wells (Carrell K. D., 1987; Frenier & Ziauddin, 2008).

After the squeeze treatment and subsequent overnight shut-in the production is resumed, and the scale inhibitor will be washed out of the formation with the produced fluids. With this throughput of formation fluids, the localized concentration of scale inhibitors begins to drop. When the inhibitor concentration drops below a certain threshold, referred to as the minimum inhibition concentration (MIC), scale inhibition is no longer effective, and the treatment must be repeated. Scale inhibitor treatment is expensive in terms of material, equipment, labor, and lost revenue from halting production. It is therefore highly beneficial to extend the treatment lifetime.

Scale inhibition treatment lifetime is highly dependent on the rate and volume of produced fluids after treatment. For a given treatment size, higher throughput and large volumes of produced fluids typically translate into shorter lifetimes when referenced on a time scale. Therefore, we use the pore volumes (PV) produced as a quantitative measure of treatment lifetime rather than total elapsed time. The treatment lifetime is the number of pore volumes injected through a given reservoir analog section when scale

inhibitor concentration drops below the minimum inhibition concentration. At this point, scale formation is likely to occur.

Two primary issues arise during the use of scale inhibitors. Firstly, after the injection of scale inhibitors, 80-90% of the injected scale inhibitor is produced out of the formation within days of resuming production (Poynton, Tidswell, & Steele, 2000). As a result, large treatment volumes are required to achieve the desired treatment lifetime. Secondly, large treatment volumes result in a long flow-back time of the injected solution, which defers hydrocarbon production and can damage to the near-wellbore area. (Shuler, 1994).

The second most detrimental impact of scale inhibitor fluid injection is the formation of psuedoscale (Baugh, Lee, & Winters, 2012). Pseudoscale is the precipitation of scale inhibitor particles when coming into contact with the metal ions in the formation brine (e.g. magnesium and calcium). Therefore, it is important to ensure that the scale inhibitor itself is compatible with the field brine.

The most effective ways to increase the treatment lifetime are to firstly increase the amount of scale inhibitor retained after the injection flood, and to secondly control the scale inhibitor release mechanism. There have been several proposed methods to increase the scale inhibitor retention, including pretreatment of reservoir rock for increased adsorption (Chen, Vikane, & Asheim, 2006; Selle, Wat, & Vikane, 2003). However, this approach is substantially more expensive than a single-stage treatment, and the approach involves longer shut-in periods. This also introduces an extra level of complexity in an uncertain system, and is not guaranteed to function as desired.

Another approach is referred to as a "precipitation squeeze treatment." In this approach low solubility scale inhibitors are complexed with divalent ions (Ca^{2+} or Zn^{2+}), where slow dissolution leads to longer treatment lifetimes (Kelland, 2009; Yuan, Sorbie, & Todd, 1993). However, this method can cause near-wellbore damage due to injected particulates.

Using encapsulated scale inhibitors (ESI's) is an alternative approach similar to the complexed scale inhibitor method mentioned previously. In this approach solid particles are impregnated with scale inhibitors (Hsu, Al-Zain, & Raju., 2000; Martins, Kelly, & Lane, 1992). These compounds rely on a mechanism of delayed or gradual release of the scale inhibitor to increase the treatment lifetime. The ESI's are hollow particles with polymeric shells that allow for the slow release of encapsulated scale inhibitor particles. Porous ceramic proppants impregnated with scale inhibitors can be pumped with the regular proppant during hydraulic fracturing operations. After the well is returned to production, the produced brine slowly dissolves the impregnated scale inhibitor. The main drawback of this approach is that the particle sizes are on the order of microns or millimeters and are therefore not suitable for unconventional or tight shale formations.

1.2 Scale Formation Mechanisms

A concise description of crystal growth and nucleation can be found in various physical and surface chemistry textbooks. The text in this section is summarized from the literature by Wiley-VCH (**Huddersman, 2012**).

1.2.1 Induction and Nucleation

The formation of a new crystalline entity from a solution starts through the nucleation process. Nucleation is the atomic or molecular processes by which the atoms or molecules of a reactant phase rearrange into a cluster of the product phase large enough as to have the ability to grow irreversibly to a larger size (**Huddersman, 2012**). The nucleus or critical nuclei are referred to as a cluster.

Nucleation can be homogenous or heterogeneous in solution. Both types are collectively knowns as primary nucleation. Secondary nucleation takes place when the nucleation is induced by the presence of crystals of the same substance.

The driving force needed for the nucleation and growth of a crystal is referred to as supersaturation and is defined as the difference in chemical potential between a molecule in solution and that in the bulk of the crystal phase.

$$\Delta\mu = \mu_s - \mu_c$$

In the above equation μ_s is the chemical potential in solution and μ_c is the chemical potential of the molecule in the bulk crystal. Following thermodynamics, the above equation can be expressed as

$$\Delta\mu = kT \ln(S)$$

where k is the Boltzmann constant, T is the absolute temperature, and S is the supersaturation ratio. When $\Delta\mu > 0$ the solution is said to be supersaturated, meaning

that nucleation and/or growth is possible, whereas when $\Delta\mu < 0$ the solution will be undersaturated and dissolution will take place. The form of the supersaturation ratio will change depending on the system considered. For nucleation and growth from solutions:

$$S = \frac{\Pi a_i^{n_i}}{\Pi a_{i,e}^{n_i}}$$

where n_i is the number of ith ions in the molecule of the crystal, and a_i and $a_{i,e}$ the actual and equilibrium activities of the ith molecule in the crystal.

The work necessary to form a cluster of n number of molecules is the difference between the free energy of the system in its final and initial states plus a term for the interface between the nucleus and solution.

$$\Delta G_T = -n\Delta\mu + 4\pi * r^2\sigma$$

In the above equation, r is the radius of the nucleus and σ is the surface free energy. If each molecule in the crystal occupies the volume, V, the equation can be expanded as:

$$\Delta G_T = -\frac{4}{3}\pi * \frac{r^3}{V}\Delta\mu + 4\pi * r^2\sigma$$

There exists a point ΔG^*, the energetic barrier that needs to be surpassed to achieve nucleation. The value of r at this point is referred to as r^*, the critical radius or nucleus size can be expressed as:

$$r* = \frac{2\sigma * V}{kT \ln(S)}$$

The value of r^* and ΔG^* decrease as the supersaturation increases. In simple terms, the chance of having nucleation in a system will be higher with higher supersaturation.

The rate of nucleation can be expressed as an Arrhenius-type equation:

10

$$J = A \exp\left(\frac{-\Delta G *}{kT}\right)$$

where A also depends on supersaturation. J represents the number of nuclei formed per unit time per unit of volume. The nucleation rate is approximately zero until a critical value of supersaturation is achieved, after which the rate increases exponentially. This critical supersaturation, expressed as $\Delta\mu_c$, defines the zone where crystal growth can proceed without additional subsequent nucleation.

1.2.2 Crystal Growth

Crystal growth is the series of processes by which an atom or molecule is incorporated into the surface of a crystal, causing an increase in size (Huddersman, 2012). The different processes can be summarized into four steps:

1. Transport of atoms through solution

2. Attachment of atoms to the surface

3. Movement of atoms on the surface

4. Attachment of atoms to edges and kinks

The first process is the "transport process," and the second through the fourth processes are referred to as "surface processes." Since these different steps normally occur in series, the slowest process will control the overall crystal growth. Therefore, growth can be transport or surface-controlled.

1.2.3 Surface Deposition

Crystal growth can be envisioned as a surface made of cubic units that form layers. Each of these layers is limited by steps or edges that contain kinks along their length. The area between steps is referred to as a terrace, and it may contain single

11

adsorbed growth units, clusters, or vacancies. Growth units attached to the surface will form one bond, whereas those attached to stops and kinds will form two and three bonds. Therefore, kink sites will offer the most stable configuration. Growth will then proceed by the attachment of units to kink sites in steps. The kink will move along the step producing an advancement of the step until this step reaches the face edge. A new step will be formed by the nucleation of a new growth unit. The process can be seen in Figure 5. Other models of nucleation and crystal growth exist, but are not covered in detail in this section.
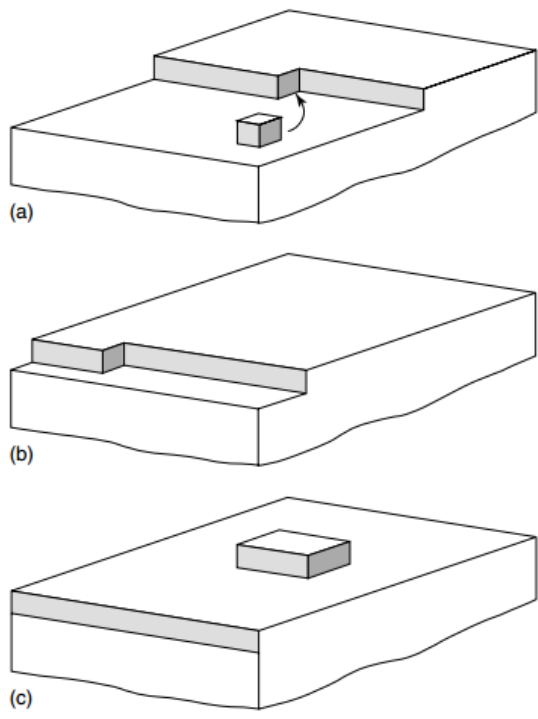
Figure 5: Schematic Representation of Layer Growth. (a) Incorporation of Growth Units Into Step. (b) The Step Has Nearly Advanced to the Edge of the Crystal. (c) Formation of a New Nucleus. (Huddersman, 2012)

12

1.3 Industry Scale Inhibitors

In order to slow or prevent scale formation, considerable efforts have been made to seek suitable chemical inhibitors (Qingfeng, 2006; Pedenaud, Goulay, Pottier, Garnier, & Gauthier, 2006; Li, et al., 2006; Tomson, Kan, & Fu, 2004). Recently, copolymer scale inhibitors have attracted interest since they have several functional groups which show the inhibition properties for different types of scale (Zhang, Wu, Hao, & Liu, 2007). Carboxyl, acrylamide, phosphonate, and sulfonate groups possess positive scale inhibition properties and have been used in industrial applications for scale and corrosion control.

Chemical scale control is dividided into three primary categories: removal acids, sequestrant, and dissolvers and scale inhibitors. Acidizing of calcium carbonates is the most prominent method of flow assurance. The major downside is that it does not stop the problem from recurring, and it does not remove precipates that are insoluble in acids such as barium sulphate (Bonnett, Fieler, & Hen, 1991; Smith, Nolan, & Crenshaw, 1968; Vetter, 1976).

Sequestrants and scale dissovlers are the second most common approach used in oildfield operations scale control. A common chemical used is reffered to as EDTA (Ethylenediamine tetraacetic acid), which has shown limited productivity improvement in some cases (Charleston, 1968; Shaughnessy & Kelly, 1983). The poor results may be due to EDTA having a poor surface-to-bulk ratio in tubular environments, which led to slow rates of dissolution (Carrell C. , 1987; Mazzoline, Bertrro, & Truefitt, 1990; Vetter, 1976).

The use of chemical scale inhibitiors is the third approach to deal with scale control. Scale inhibitors act as crystal distortion reagents within the reservoir. This is achieved primarily by adsorption of the scale inhibitor onto the active growth sites of the scale crystal (initial scale nucleation), leading to changes in the crystal morphology, thereby retarding crystal growth and further nucleation. Scale inhibitors have been widely used to control scale formation by repeated injection of these chemicals into the formation. The treatments are repeated as necessary to protect surface equipment and downhole operations. These applications are commonly referred to as "squeeze treatments." Ever since early attempts showed promise of succesful prevenative measures for continued flow assurance, use has been widespread in the oilfield industry.

Downhole squeeze treatments for scale control initially were developed with a focus on principally preventing scale formation. In order to improve the performance of commercial scale inhibitors, a new focus has been to develop chemicals with high adsorption and retention in formation rock. The success of squeeze treatments are dependent on having both high scale inhibition properties (with an MIC in the 5 to 15 ppm range) and an intrinsic ability to be retained in the formation. After squeeze treatments the scale inhibitor lifetime is measured in terms of throughput. Laboratory experiments measure treatment lifetime in terms of pore volume (PV). In the field, it can be approximated in terms of barrels produced and correlated to a measure of time. Typically, commercial treatment lifetimes may vary from 250 Mbbl to 300 Mbbl, and can last from anywhere from 3 months to 12 months (Ibrahim, Sorbie, & Boak, 2012).

There are many concerns, however, when working with scale inhibitors: dealing with high temperature applications can impact the chemistry of compounds, the inherent toxicity of chemicals, and the inclusion of functional groups for brine compatibility with the formation. Conventional polymer and phosphonate scale inhibitors may not be appropriate for application in high pressure and high temperature applications. Only a limited range of commercially available oil field scale inhibitor chemicals are sufficiently stable at temperatures up to and above 150 ºC (Fink, 2003). These chemicals are homopolymers of vinyl sulfonate and copolymers of acrylic acid and vinyl sulfonate. Other polymers, such as polymaleic acid, polyitaconic acid, and maleic acid/acrylic acid copolymers, may offer similar thermal stability.

This research project will primarily focus on copolymers of acrylic acid, the primary component for scale inhibition, the inclusion of a sulfonate group, which is present primarily for brine compatibility. By utilizing a cross-linked polymer, we can control the size of the NSI, and no surfactant would be required for stability in brine.

1.4 Mission

1.4.1 Current Issues with Scale Inhibitors

Inhibitors easily wash out due to low retention/weak adsorption to rock surface. Some inhibitors can be toxic to flora and fauna (e.g. phosphonate inhibitors). Delivery into the wellbore can often be difficult and costly. Inhibitor-loaded nano/macro-particles can precipitate before reaching the targeted areas.

1.4.2 Project Goals

The purpose of this project is firstly to develop a synthesis recipe for a novel nanoized scale inhibitor with high brine compatibility, high inhibition efficiency, and high retention in the reservoir. An additional aim is to improve upon the current treatment lifetime over the current state-of-the-art products. Also, it is desirable that the nanoized scale inhibitor functions adequately with particle sizes in the nanometer range. Therefore, scale inhibitor should be suitable for applications in both formation rock and fractures.

Once the synthesis of products has proved to be repeatable and the copolymers have adequate brine compatibility, this project will investigate the minimum inhibition concentration (MIC) over time. We will use a model brine containing the divalent atoms (e.g. calcium, strontium, barium ions) which lead to troublesome scale formation. Our scale inhibitor will function on a delayed-release mechanism controlled by hydrolysis (rather than dissolution). The investigation of MIC versus time will yield the release profile of the scale inhibitor.

Quartz Crystal Microbalance with Dissipation (QCM-D) studies will be performed in order to investigate the electrostatic adsorption of the NSI to various surfaces. This information will identify to what extent electrostatic interactions play a part in the overall retention mechanism in our system.

Finally, dynamic retention studies will be performed with a sand pack. Scale inhibitor injection (squeeze) trials will be performed with subsequent flow-through of the model brine in order to investigate the scale inhibitor retention under reservoir-like

conditions. Two factors will primarily influence the performance of the NSI. The first is the dynamic retention in porous rock, and second is the hydrolysis-controlled release mechanism of the scale inhibitor from the nanoized particle. If these two factors can be maximized, then the treatment lifetime of the NSI should be less influenced by throughput than current state-of-the-art products, which function on dissolution. Ideally, this will result in less frequent treatment requirements in production wells.

2. SYNTHESIS OF SCALE INHIBITOR AND ANALYSIS OF BRINE COMPATIBILITY
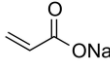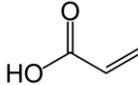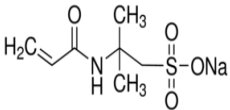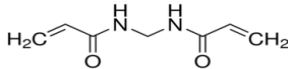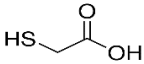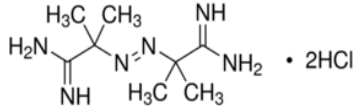
2.1 Objective

This section will detail attempts to develop a repeatable synthesis recipe for a novel scale inhibitor. Additionally, we will study the brine compatibility under reservoir temperatures for long durations.
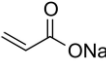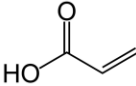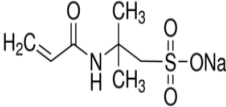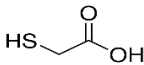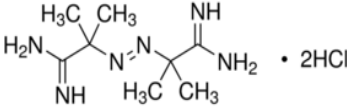
2.2 Materials and Methods

Several attempts were made at establishing an ideal recipe for the scale inhibitor synthesis. The procedure detailed below is what was proved to be successful over repeated attempts. All components of the synthesis can be seen in Table 2 and Table 3, below. Model brine and synthetic seawater recipes can be found in Table 4 and Table 5.

Table 2: List of Reagents for Cross-Linked Scale Inhibitor Synthesis

Name	Function	Structure	Supplier
Sodium acrylate (SA)	Scale Inhibitor		Sigma-Aldrich
Acrylic acid (AA)	Scale Inhibitor		Sigma-Aldrich
2-Acrylamido-2-methyl-1-propanesulfonic acid sodium salt (50%) (AMPS)	Brine Compatibility Agent		Sigma-Aldrich
N,N′-Methylenebis(acrylamide)	Cross-Linker		Sigma-Aldrich
Thioglycolic acid	Chain Transfer Agent		Sigma-Aldrich
2,2′-Azobis(2-methylpropionamidine) dihydrochloride (VAZO 56)	Initiator		Sigma-Aldrich
Hydrochloric acid	pH balance	HCl	Sigma-Aldrich
Water	Solvent	H_2O	-

Table 3: List of Reagents for Linear Scale Inhibitor Synthesis

Name	Function	Structure	Supplier
Sodium acrylate (SA)	Scale Inhibitor		Sigma-Aldrich
Acrylic acid (AA)	Scale Inhibitor		Sigma-Aldrich
2-Acrylamido-2-methyl-1-propanesulfonic acid sodium salt (50%) (AMPS)	Brine Compatibility Agent		Sigma-Aldrich
Thioglycolic acid	Chain Transfer Agent		Sigma-Aldrich
2,2′-Azobis(2-methylpropionamidine) dihydrochloride (VAZO 56)	Initiator		Sigma-Aldrich
Hydrochloric acid	pH balance	HCl	Sigma-Aldrich
Water	Solvent	H_2O	-

Table 4: Model Brine Recipe - Model Anion is Prepared Beforehand Without Sodium Bicarbonate Due to its Natural Tendency to Break Down Over Time in Solution. Sodium Bicarbonate is Added on the Day of Use.

Model Brine Recipe			
Anion	Wt. (g/Kg)	Cation	Wt. (g/Kg)
Na_2SO_4	0.931	$MgCl_2*6H_2O$	4.3155
NaCl	18.3839	$SrCl_2*6H_2O$	0.5899
$NaHCO_3$	0.694	BaCl2	0.0756
$NaAc*3H_2O$	0.5927	$CaCl_2*2H_2O$	7.1894
		KCl	0.5095
		NaCl	18.384
Total	20.6	Total	31.1
Combined Total Wt. Salts = 25.85 g/Kg water			

Table 5: Synthetic Seawater Recipe – The Solution is Prepared Beforehand Without Sodium Bicarbonate Due to its Natural Tendency to Break Down Over Time in Solution. Sodium Bicarbonate is Added on the Day of Use.

Synthetic Seawater	
Component	Wt. (g/kg)
NaCl	26.518
KCl	0.725
$CaCl_2*2H_2O$	1.141
$MgCl2*6H_2O$	2.447
NaBr	0.083
$MgSO_4$	3.305
$NaHCO_3$	2.02
Total	36.239

Scale Inhibitor Synthesis Procedure

The following is the procedure for preparing the cross-linked scale inhibitor. The same procedure can be followed for linear scale inhibitor preparation with the removal of the cross-linker and the sole use of acrylic acid (rather than a 50/50 mix of acrylic acid and sodium acrylate). The overall procedure is represented schematically in Figure 6.

1. Prepare a round bottom flask of adequate size for desired batch size. Prepare a stir bar approximately 75% in length of the diameter of the round bottom flask.

2. Prepare a rubber stopper, hose clamp, long steel needle, and nitrogen gas tank for later use.

3. Calculate the proper molar ratios of sodium acrylate/acrylic acid to AMPS.

    a. For brine compatibility checks, we will prepare 0-30mol% AMPS (of total monomers). These three components will comprise ~12% wt. of the bulk mixture.

4. Add ~20% of total desired water content to round bottom flask.

5. Add thioglycolic acid, acrylic acid, and methylene bisacrylamide to round bottom flask, in that order. Record all masses.

6. Dissolve all solids by ultra-sonication in the flask until solution is uniform.

7. Add AMPS, sodium acrylate, and VAZO 56 to round bottom flask. Record all masses.

8. Dissolve all solids by ultra-sonication in the flask until solution is uniform.

9. Prepare HCl solution of ~18% wt. solution in DI water. Add HCl solution dropwise until the pH has reached 3.75. It is at this pH that the rates of polymerization for all monomers are approximately equal. Record all masses.

10. Add water to reach final total volume desired.

11. Cap the round bottom flask with the rubber stopper, and tighten hose clamp for air-tight seal. Insert the steel needle until submerged in the solution. Insert syringe needle to allow ventilation. With stirring, purge the vessel with nitrogen gas for 15 minutes. Prepare a hot water bath at 60 ºC.

12. After the purge with nitrogen gas, remove the steel needle and syringe needle to ensure a closed system. Place the round bottom flask in the water bath with stirring at ~150 rpm.

13. Set a timer for 3 hours. Observe gelation time.
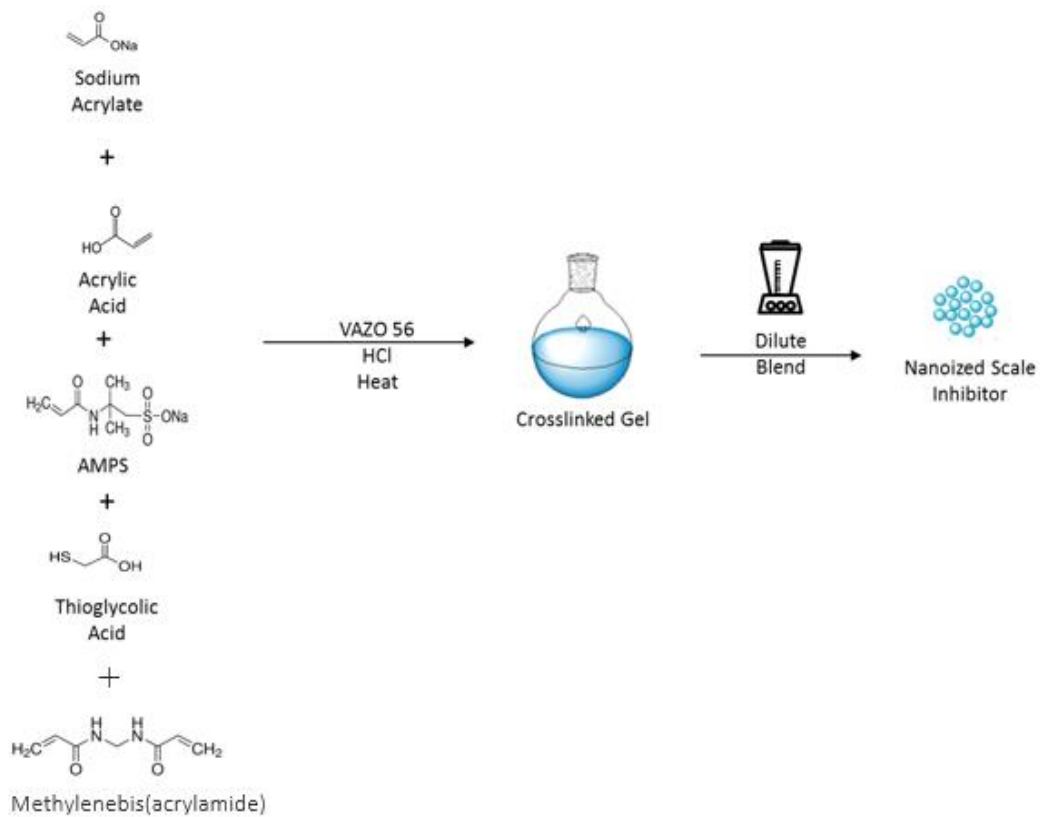
Figure 6: Schematic Representation of Preparation of Scale Inhibitor

<h1 align="center">Brine Compatibility Check Procedure</h1>

1. Prepare a 4000 ppm solution of scale inhibitor in DI water

   a. Calculate poly(sodium acrylate) (PSA) concentration in gel/solution.

$$(PSA\ wt.\%)_f = \frac{m_{SA} + m_{AA} * \left(\frac{MW_{SA}}{MW_{AA}}\right) + m_{AMPS}\left(\frac{MW_{SA}}{MW_{AMPS}}\right) + m_{XL}\left(\frac{MW_{SA}}{MW_{XL}}\right) * 2}{m_{Tot}}$$

   b. Dilute in DI water for final concentration.

$$(PSA\ wt.\%)_f = \frac{m_{SI\ soln.} * (PSA\ wt.\%)_i}{m_f}$$

2. Blend for several minutes in commercial blender on low setting. Measure particle properties (size, zeta potential) until desired characteristics are achieved.

3. Prepare model brine solutions for both anion[1] and cation. Exact mixture components can be seen in Table 4 (suggest delete all pages number. Table or figure + number is enough. When you add or delete or edit something, page number will change. So you have to change all page numbers).

4. Dilute the 4000 ppm SI solution into 1000 ppm with 50/50 mixture of model brine.

5. Aliquot 5 ml samples into glass vials with crimped cap. Place into oven at 95 ºC for at least 2 hours.

6. Observe for precipitation after incubation at 95 °C.

---

[1] Model anion is prepared beforehand without sodium bicarbonate due to its natural tendency to break down over time in solution. Sodium bicarbonate is only added on the day of use.

2.3 Results and Discussion

A series of scale inhibitor samples were firstly synthesized with different AMPS content. The synthesis recipes for selected batches can be seen in Table 6. The data are shown to give the reader a perspective on the relative amounts of each reagent for the syntheses. The 10-30mol% AMPS range was selected for representation as a result of the brine compatibility results, which are discussed later in this section.

Table 6: Synthesis Recipes for Brine Compatibility Experiments

Reagents	AMPS, Mol %				
	10	15	20	25	30
Sodium Acrylate, g	3.91	1.33	11.28	11.78	10.99
Acrylic Acid, g	1.93	1.02	8.65	9.03	8.42
50wt% AMPS, g	3.49	2.24	26.79	37.28	44.74
Methylene Bisacrylamaide, g	1.45	0.73	5.50	7.32	7.32
Thioglycolic Acid, g	0.59	0.29	2.24	2.94	2.94
H_2O, g	56.13	33.37	240.43	223.33	217.26
VAZO 56, g	0.67	0.33	2.50	3.33	3.33
HCl + Water (pH = 3.75), g	-	0.50	2.62	5.00	5.00

A range of recipes ranging from 0-30mol% AMPS were synthesized. (Molar percentages 0-30 mol% means AMPS content of total monomers.) Each synthesis batch was diluted to 1000 ppm scale inhibitor concentration in model brine, aliquoted into glass vials, capped, and placed into an over at 95 °C for several hours. The vials were then removed from the oven and observed for precipitation. The results are summarized in Figure 7 and Table 7.

26
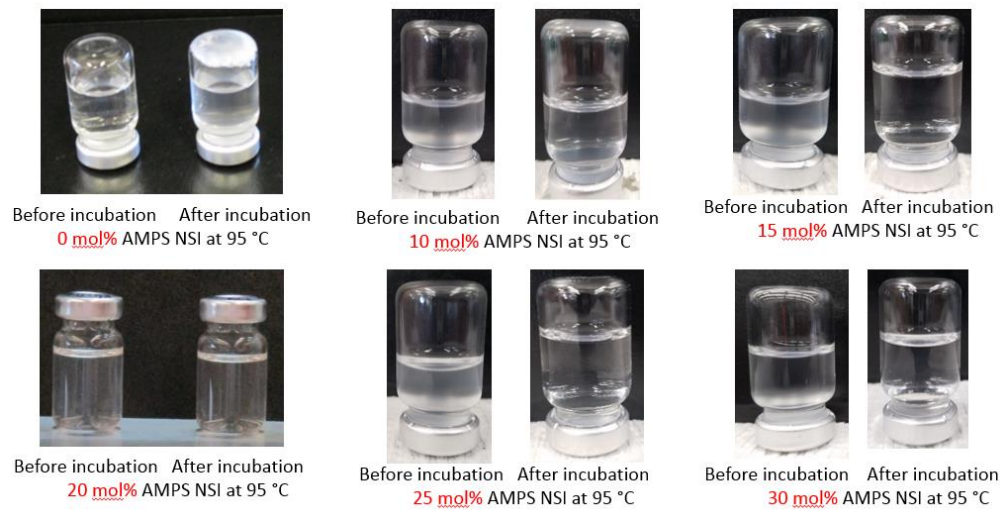
Figure 7: Samples of Various AMPS: (SA/AA) Ratio Before and After Incubation at 95 ºC

Table 7: Brine Compatibility Results for Various Scale Inhibitor Recipes

Batch	1	2	3	4	5	6
AA/SA, (mol%)	100	90	85	80	75	70
AMPS, (mol%)	0	10	15	20	25	30
Compatibility with model brine	No	No	Yes	Yes	Yes	Yes

As we can see, synthesis of cross-linked scale inhibitor with 100% acrylate components (SA/AA) forms a precipitate after incubation at 95 ºC. Of the six samples that were observed, only the 15%-30% AMPS NSI samples were brine compatible. Brine compatibility appears to increase with increasing AMPS content, and it is evident

27

from the data that any recipe containing less than 15% AMPS content will precipitate out of solution, and these are therefore inadequate for further study as an applicable solution for scale control.

2.4 Synthesis and Brine Compatibility Conclusions

At this stage of the project, we have developed a successful, repeatable synthesis recipe and procedure. Additionally, we have found a range of molar percentage AMPS where we have a brine-compatible solution. This is extremely important to ensure scale inhibition under reservoir conditions without the formation of psuedoscale. It is also important to consider the functions of each of these components: the acrylate group is our scale inhibition component, and the sulfonate group is for brine compatibility. We want to balance these two functions, while maximizing our scale inhibition performance. We will exclude the 30% AMPS because this is the higher end of the spectrum. That is, the higher molar percentage of AMPS decreases the amount of scale inhibitor in our final product. In the subsequent studies, we will continue with the 15-25% AMPS range.

3. MINIMUM INHIBITION EFFICIENCY

The previous section details the synthesis of the scale inhibitor. This section focuses on the experimental observation of the inhibition efficiency over time. Varying ratios of AMPS: (SA/AA) are prepared and observed in order to generate the release profile and observe the MIC over time.

3.1 Objective

The purpose of this section is to measure the minimum inhibition concentration (MIC) of the scale inhibitor mixed with synthetic formation brine stored at reservoir temperature over time. Measuring the turbidity of the solutions will be the primary analytical tool. Several samples of any given synthesis batch will be stored at high temperatures and anaerobic conditions. Samples will be periodically removed for analysis, and aggregation of the data will yield the release profile. High temperatures in solution will lead to hydrolysis of the cross-linked particle, and the decrease in the MIC over time will function as the indicator of the release of more scale inhibitor from the cross-linked polymer.

3.2 Materials and Methods

MIC Sample Incubation Procedure

1. Place oxygen (O_2) scrubber plates into an oven at 90 $^{\circ}$C. This is to release any bound O_2 from the plates.

2. Prepare a 4000 ppm solution of scale inhibitor in DI water

    a. Calculate poly(sodium acrylate) (PSA) concentration in gel/solution.

29

$$(PSA\ wt.\%)_f = \frac{m_{SA} + m_{AA} * \left(\frac{MW_{SA}}{MW_{AA}}\right) + m_{AMPS}\left(\frac{MW_{SA}}{MW_{AMPS}}\right) + m_{XL}\left(\frac{MW_{SA}}{MW_{XL}}\right) * 2}{m_{Tot}}$$

      b. Dilute in DI water for final concentration.

$$(PSA\ wt.\%)_f = \frac{m_{SI\ soln.} * (PSA\ wt.\%)_i}{m_f}$$

3. Blend for several minutes in commercial blender on low setting. Measure particle properties (size, zeta potential) until desired characteristic are achieved.

4. Prepare model brine solutions for both anion[2] and cation. Exact mixture components can be seen in Table 4.

5. Dilute the 4000 ppm SI solution into 1000 ppm with 50/50 mixture of model brine.

6. Prepare 10 glass vials and crimped caps (label each vial with SI contents). Move beaker with 1000 ppm SI solution in brine, 10 glass vials with caps, a small vial with DI water, and O_2 scrubber plates to the anaerobic transfer vessel. Include all necessary pipettes for fluid transfer in the chamber. Purge vessel with N_2 and Ar cycling.

7. Transfer all contents into anaerobic chamber and place fresh O_2 scrubber plates over fans for air circulation.

---

[2] Model anion is prepared beforehand without sodium bicarbonate due to its natural tendency to break down over time in solution. Sodium bicarbonate is only added on the day of use.

8. Mass the beaker of SI solution. Then place the beaker on a plate with stirring for ~10 minutes while O_2 levels drop to nearly 0 ppm. Uncap the vial with DI water and place to the side for the duration.

9. Place the beaker on a balance and add DI water with a pipette to compensate for mass lost.

10. Use a pipette to transfer 5 ml of SI solution into each glass vial. Crimp a cap onto each vial.

11. Place vials on a metal tray, and place the tray into the oven at 90 °C.

12. At selected intervals (e.g. once each week) measure the minimum inhibition concentration.

<div align="center">MIC Check Procedure</div>

1. On the desired day of examination (day 0 to day ~60), remove 1 vial of the sample from the oven. For day 0 examination, use freshly prepared sample.

2. Prepare a water bath on a hot plate with a magnetic stirring capability. Set to ~95 °C with ~1000 rpm stirring.

3. Prepare stock solutions of model anion and cation. Exact mixture components can be seen in Table 4.

4. Prepare 3, 30 mL glass vials with screw caps. Prepare three dilution stock solutions from the 1000 ppm stock solutions according to Table 8. Fluid mixtures will be measured gravimetrically.

Table 8: MIC Stock Solution Preparation

Desired Concentration (ppm)	Component	Desired Mass (g)
100	1000 ppm SI Soln.	2
	Anion	9
	Cation	9
20	100 ppm SI Soln.	4
	Anion	8
	Cation	8
5	20 ppm SI Soln.	5
	Anion	7.5
	Cation	7.5

5. Prepare 10 glass vials with crimped caps. Use sample stock solutions prepared in the previous step to prepare the experimental samples according to Table 9.

Table 9: MIC Sample Preparation

Desired Concentration (ppm)	Component	Desired Mass (g)
50	100 ppm SI Soln.	2.5
	Anion	1.25
	Cation	1.25
10	20 ppm SI Soln.	2.5
	Anion	1.25
	Cation	1.25
4	20 ppm SI Soln.	1
	Anion	2
	Cation	2
3	5 ppm SI Soln.	3
	Anion	1
	Cation	1
2	5 ppm SI Soln.	2
	Anion	1.5
	Cation	1.5
1	5 ppm SI Soln.	1
	Anion	2
	Cation	2
0	Anion	2.5
	Cation	2.5

6. Add a stir bar to each vial, cap each vial, and suspend each vial in hot water bath such that there is adequate stirring in each container.

7. Set a timer for 2 hours and incubate. Refill water bath as necessary. Verify that water temperature is 95 ⁰C throughout. Prepare UV-Vis spectrometer for sample analysis.

8. After 2 hours has elapsed, removed samples from water bath. As quickly as possible, move samples to UV-Vis Spectrometer area.

9. Use DI water as a blank. Measure the absorbance (turbidity) of each sample at 500 nm wavelength. Record all results.

<div align="center">Experimental Equipment</div>

An anaerobic chamber with attached airlock was used to purge the samples of oxygen, and samples were housed within ovens contained within the anaerobic chamber. The setup can be seen in Figure 8.

Figure 8: Anaerobic Chamber Containing a Stirring Plate, Mass Balance, High Temperature Ovens, Condensation Catalyst, Circulation Fan, and H_2/O_2 Detector

A Cary 60 UV-Vis Spectrophotometer made by Agilent Technologies was used to measure the turbidity (i.e. absorbance) of each sample. The instrument can be seen in Figure 9.
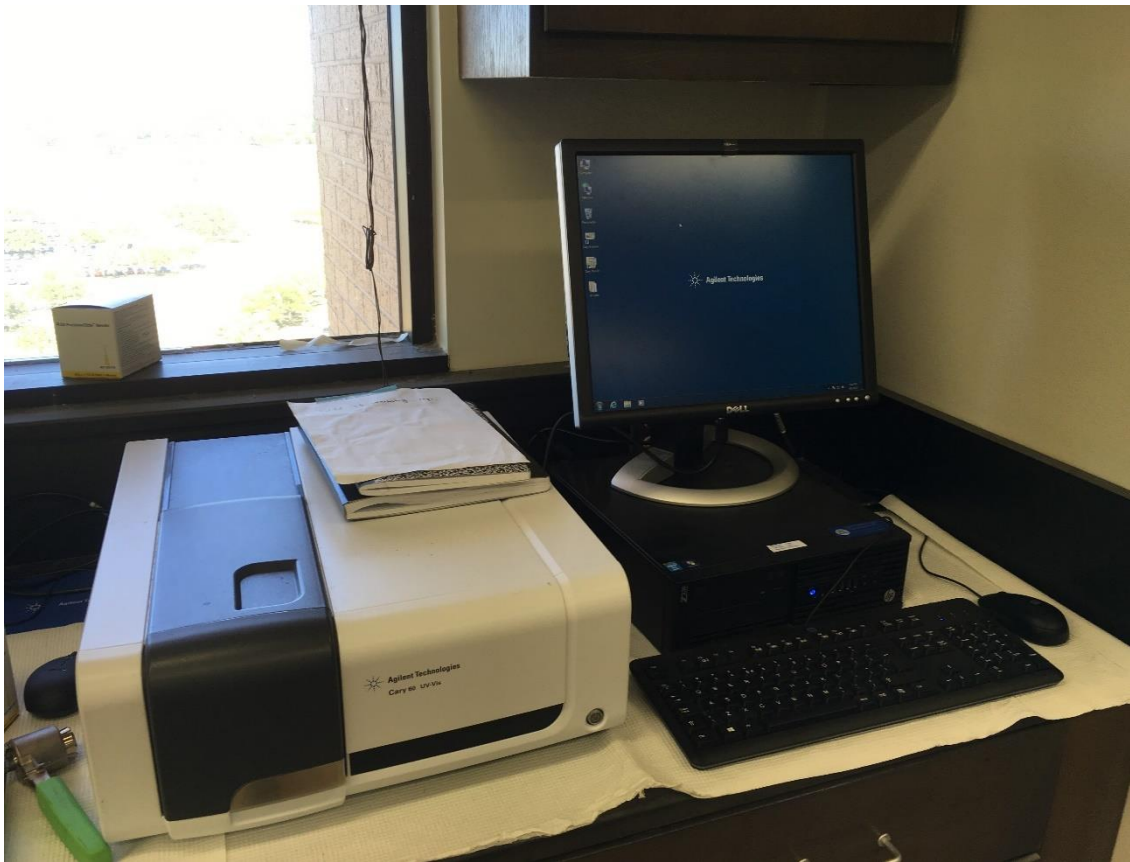
Figure 9: Cary 60 UV-Vis Spectrophotometer by Agilent Technologies

Particle size and zeta potential measurements were done using a NanoBrook Omni particle sizer and zeta potential analyzer manufactured by Brookhaven Instruments Corporation. The instrument can be seen in Figure 10.

Figure 10: NanoBrook Omni Particle Sizer and Zeta Potential Analyzer by Brookhaven Instruments Corporation

3.3 Results and Discussion

Incubation samples were prepared for 15mol%, 20mol%, and 25mol% AMPS

NSI and placed into the oven under anaerobic conditions. Vials containing the 1000 ppm

NSI samples were removed from the ovens, and diluted samples (0-100 ppm NSI) were

then incubated in model brine for 2 hours at 90 ºC. The turbidity of each sample was

then measured via UV-Vis Spectrophotometry at 500 nm wavelength. The results were

plotted to determine the MIC at various time intervals. The release profile for cross-

linked scale inhibitor can be viewed for each recipe individually.

Figure 11: Release Profile for 15mol% AMPS NSI

Figure 12: Release Profile for 20mol% AMPS NSI
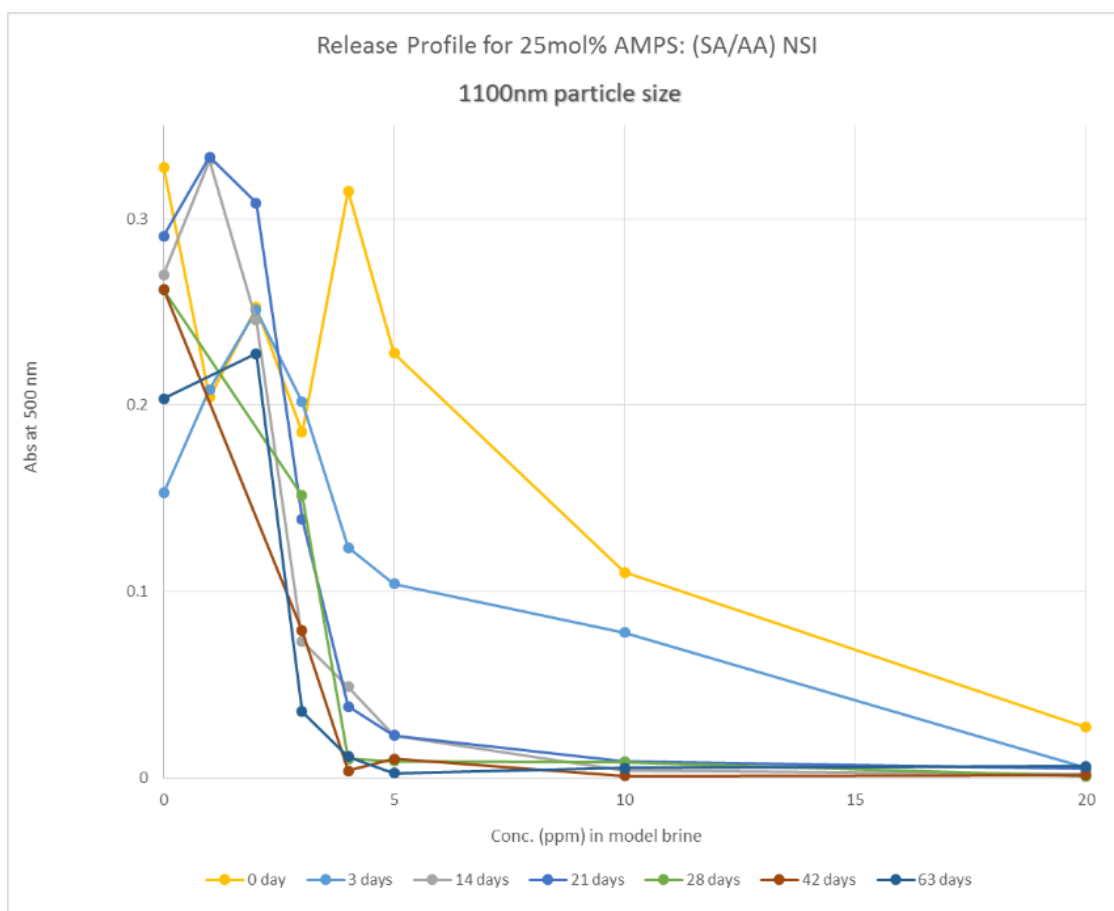
Figure 13: Release Profile for 25mol% AMPS NSI
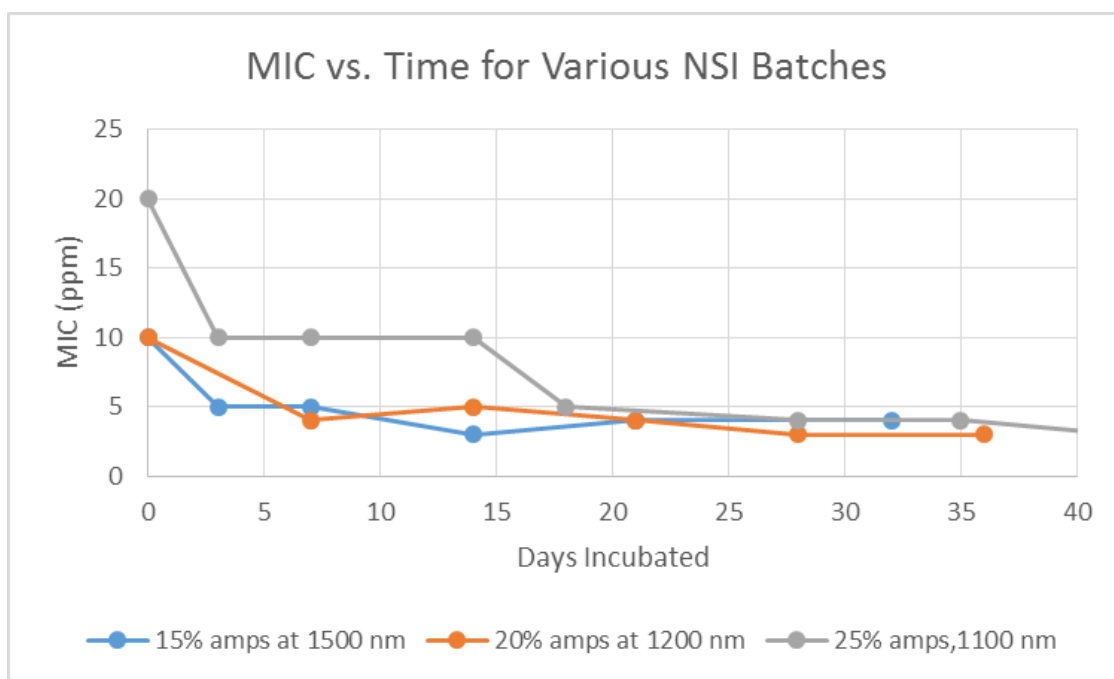
Figure 14: MIC vs. Time for Various NSI Batches

As can be seen in Figure 11 the MIC for 15mol% AMPS NSI is initially high (Day 0) at around 10 ppm and decreases to 3-4 ppm over the duration of 32 days. A similar trend holds for the 20mol% and 25mol% NSI batches. The release profiles for each batch can be seen in Figure 12 and Figure 13, respectively. The MIC for 20mol% AMPS NSI is initially high (Day 0) at around 10 ppm and decreases to 3 ppm over the duration of 36 days. The MIC for 25mol% AMPS NSI is initially high (Day 0) at around 20 ppm and decreases to 4 ppm over the duration of 35 days.

An alternative view of the data can be seen if we select the MIC points at each measurement time. The MIC plot versus time for each batch over time can be seen in Figure 14. The initial MIC for each batch can be viewed as relatively high, between 10

41

and 20 ppm. This is expected, as at time zero, the NSI particles are at their largest, and the least amount acrylate has been released into solution to complex with the divalent ions. This leads to higher initial turbidity of the solutions. Over time, hydrolysis released free acrylate components into solution, and lower MIC concentrations are achieved as time progresses. Based off of these results, we can justifiably say that the NSI has sustained release of more than 40 days duration at 95 °C.

3.4 Minimum Inhibition Efficiency Conclusions

Our scale inhibitor system shows sufficient MIC and release profile over the duration of approximately two months. At this point in the project, we will continue with one recipe for further studies. The 20mol% AMPS NSI recipe will be used in subsequent experiments. This recipe is chosen because we will have sufficient guarantee of brine compatibility while retaining a maximum molar amount of scale inhibitor components.

4. QUARTZ CRYSTAL MICROBALANCE WITH DISSIPATION STUDIES

This section details an analysis of static adsorption of our scale inhibitor to a surface. QCM-D analytical techniques use quartz sensors with various materials to simulate specific surface charges and material environments. This project utilizes silicon dioxide and gold sensors to analyze scale inhibitor interactions with negatively charged and neutral surfaces, respectively. Silicon dioxide will function as an analog to quartz sand, which has a negative surface charge. The gold sensor will be coated with polyethylenimine (PEI) in order to function as an analog to carbonate sand, which has a positive surface charge.
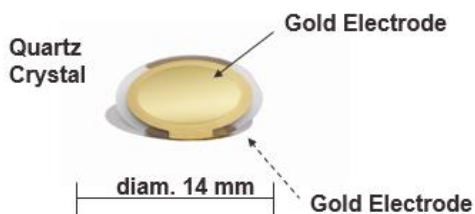
Figure 15: Top and Bottom View of QCM-D Sensor (Gold) (Dixon & BiolinScientific, 2014)

A view of a silicon dioxide sensor can be seen in Figure 15. The outer rim of the circular sensor is a quartz material, and the center of exposed surface is exposed to the particles in solution. The sensor is placed in a chamber with two electrodes opposite the exposed side, and a voltage is applied across the quartz. Quartz, behaving as a

piezoelectric material, then oscillates at a specific frequency due to the applied voltage. The resonant frequency (as well as harmonic overtones) are an intrinsic property of the sensor. As fluids are flowed across the sensor, particles interacting with the exposed surface will in turn affect the frequency of oscillation. These frequency shifts can be observed over time and correlated to mass adhering to the surface of the sensor.

Additionally, using the QCM-D analytical method we can observe the dissipation over time. Dissipation can be correlated to the rigidity of a particle in solution. The dissipation is measured via the ping principle, which is illustrated in Figure 16.
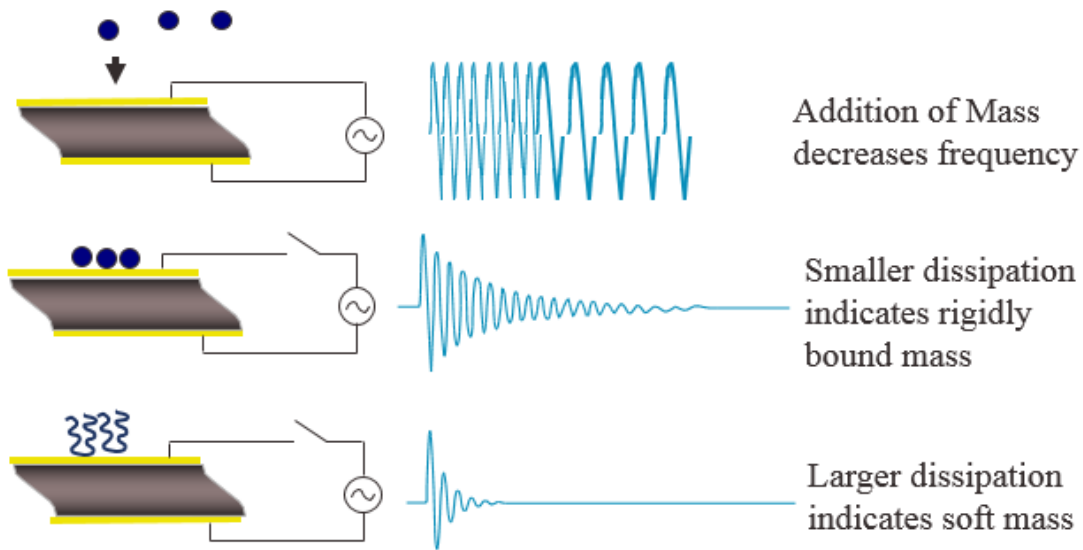
Figure 16: Illustration of the QCM-D Ping Principle (Dixon & BiolinScientific, 2014)

The resonant frequencies are first established with a standard solution, usually DI water, and particle solutions are moved over the surface using a peristaltic pump. As particles adhere to or settle upon the surface a decrease in frequency will be observed due to dampening of the signal. The QCM-D equipment will pause the application of a voltage across the surface and observe the decrease in amplitude of the frequency over time. Smaller dissipation values, which indicate a longer attenuation of the signal, corresponds to a rigid particle. Higher dissipation values, indicating a shorter attenuation of the signal, indicates a softer mass. The softer mass scenario would indicate a material which is referred to as viscoelastic.

With the frequency and dissipation signals measured over time, we can qualitatively analyze the data for electrostatic interactions with a surface and rigidity of a film adhering to a surface. The analytical technique can be used further to quantify the mass adhering to a surface. However, quantification of these parameters requires that the user know the exact physical characteristics of the particle, including density and viscosity. Quantitative interpretation will not be included in the analysis in this section.

4.1 Objective

The primary objective of the QCM-D experiments is to determine the magnitude of which our nanoscale inhibitor will bind to rock surfaces. Silicon dioxide sensors will function as our analog to quartz sand. Gold sensors will function as a neutral surface for a control comparison of electrostatic interaction. PEI-coated gold sensors will function as an analog to carbonate sand. The 20mol% AMPS scale inhibitor is used in this section in addition to the linear scale inhibitor.

45

4.2 Materials and Methods

1. Prepare a 4000 ppm solution of scale inhibitor in DI water

    i.   Calculate poly(sodium acrylate) (PSA) concentration in gel/solution.

$$(PSA\ wt.\%)_f = \frac{m_{SA} + m_{AA} * \left(\frac{MW_{SA}}{MW_{AA}}\right) + m_{AMPS}\left(\frac{MW_{SA}}{MW_{AMPS}}\right) + m_{XL}\left(\frac{MW_{SA}}{MW_{XL}}\right) * 2}{m_{Tot}}$$

    ii. Dilute in DI water for final concentration.

$$(PSA\ wt.\%)_f = \frac{m_{SI\ soln.} * (PSA\ wt.\%)_i}{m_f}$$

2. Blend for several minutes in commercial blender on low setting. Measure particle properties (size, zeta potential) until desired characteristic are achieved.

3. Prepare model brine solutions for both anion[3] and cation. Exact mixture components can be seen in Table 4.

4. Dilute the 4000 ppm SI solution into 1000 ppm with 50/50 mixture of model brine.

5. Dilute the 1000 ppm SI solution in brine into a 100 ppm SI solution with DI water. This is done (1) to have a final NSI concentration of 100 ppm and (2) to reduce the total dissolved solids content to maintain the QCM-D equipment.

6. Prepare the sensors for the scenario of choice:

    i.   Negatively charged surface: Silicon dioxide sensors

    ii. Neutral or positively charged surface: Gold sensors

---

[3] Model anion is prepared beforehand without sodium bicarbonate due to its natural tendency to break down over time in solution. Sodium bicarbonate is only added on the day of use.

i.　For positively charged surface, prepare a 1% by weight solution of

　　　　　　　　　PEI (25k Dalton) in DI water.

7.　Clean the sensors according to the Q-Sense standard operating procedures. Set

　　the sensors in the chambers.

8.　Place all fluids (DI water, PEI solution, and SI solutions) in glass containers.

　　French Square Bottles (200 mL) are recommended.

9.　Place containers in water bath and set to 45 $^{\circ}$C. Wait ~1 hour for temperature to

　　equilibrate.

10.　In the QCM-D software, connect to instrument and set the chamber temperature

　　to 45 $^{\circ}$C. Inject DI water at 50 µL/min flow rate. Wait ~1 hr for temperature to

　　equilibrate, and then establish the "zero point" resonant frequencies.

11.　Begin recording data in software interface.

12.　Wait for steady baseline with DI water flowing over surface. For Gold + PEI

　　conditions, pump 1% PEI over the gold sensors and wait ~1 hour to establish

　　stable baseline.

13.　Inject linear and cross-linked scale inhibitor solutions into the designated

　　chambers for >10 minutes or until signals stabilize.

14.　After adequate data have been collected, inject DI water for post flush.

15.　End data acquisition. Clean all sensors and chambers according to Q-Sense

　　standard operating procedures.

Experimental Equipment

A Q-Sense QCM-D E4 system was used to measure the particle-surface interactions via frequency shift and dissipation measurements. A graphical image of the system can be seen in Figure 1Figure 17. Inside the housing chamber, four individual sensor chambers are located where they are mounted to a common aluminum baseplate for equal and efficient temperature control. An image of the housing can be seen in Figure 18.

Figure 17: Q-Sense QCM-D E4 System (mrqsense, 2009)
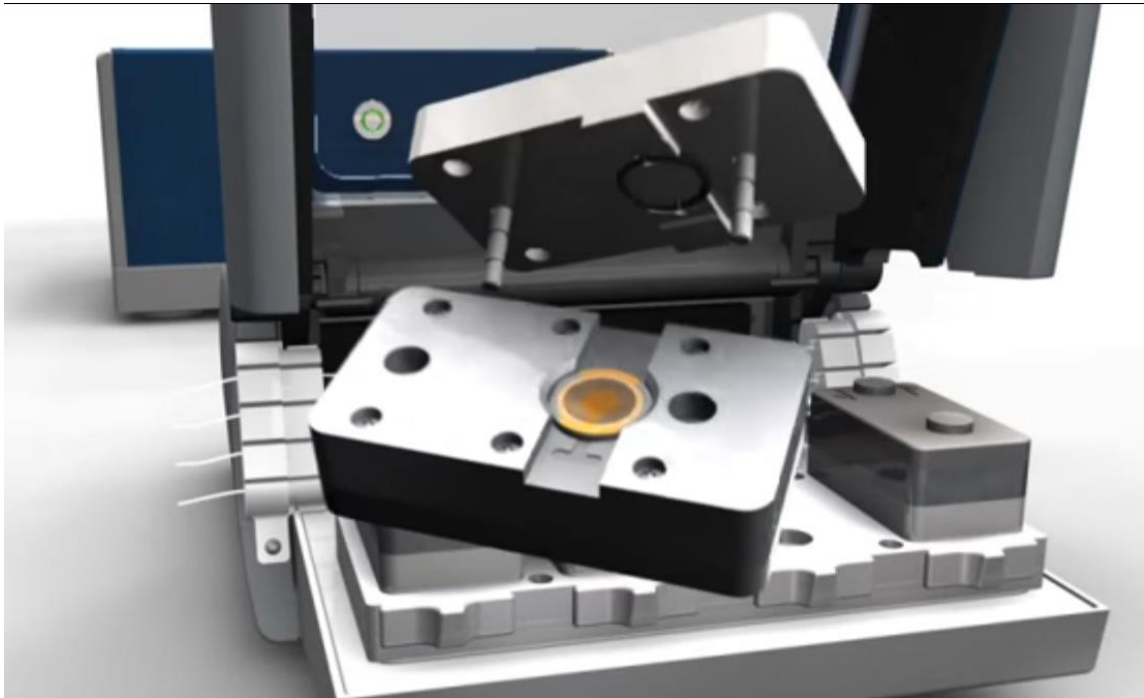
Figure 18: Sensor and Sensor Chamber in QCM-D Equipment (mrqsense, 2009)

Particle size and zeta potential measurements were done using a NanoBrook Omni particle sizer and zeta potential analyzer manufactured by Brookhaven Instruments Corporation. The instrument can be seen in Figure 10.

4.3 Results and Discussion

Silicon dioxide sensors were prepared, and the linear and cross-linked scale inhibitor (NSI) were injected over the sensors. The SiO_2 sensors are negatively charged and function as our quartz sand analog. The experiments utilizing the gold sensors were conducted on a separate day. The gold sensor alone was used as the neutral condition, and the 1% PEI solution was used to coat 2 of the 4 sensors to create a positively charged surface. The gold + PEI sensors function as our carbonate sand analog. The

scale inhibitor solutions were prepared, and the particle properties were measured. The particle properties can be seen in Table 10.

Table 10: Scale Inhibitor Particle Properties for QCM-D Experiments

Experiment Conditions	Scale Inhibitor	Particle Size (nm)	Zeta Potential (mV)
SiO2 (-)	Linear	-	-15.98 ± 2.88
	Cross-Linked	297.81 ± 7.57	-7.89 ± 3.17
Gold	Linear	-	-9.14 ± 6.08
	Cross-Linked	294.89 ± 6.51	-13.41 ± 5.38
Gold + PEI (+)	Linear	-	-9.14 ± 6.08
	Cross-Linked	294.89 ± 6.51	-13.41 ±5.38

The experiments were performed on different time scales due to the desired conditions. That is, the gold and gold + PEI conditions required more time to come to equilibrium.

When qualitatively interpreting the data, we primarily look for three things: the degree of change before and after injecting new fluids, flatness of signal response, and the degree of overlap (or deviation) of the harmonic signals. The degree of change in the frequency signal is an indication of the relative amount of mass adhering to a sensor. Flat signal response is an indication of steady-state. Signal overlap is an indication of rigid-film behavior, whereas deviation in the signal is an indication of viscoelastic behavior.

We first examine the interactions of the linear scale inhibitor across all three conditions. The frequency drop data for the linear scale inhibitor can be seen in Figure

19. There are three curves shown in this visualization for each condition. Each of these curves corresponds to the 5th, 7th, and 9th harmonics. These harmonics were chosen because they had the cleanest response signals, and they adequately represent the spread in the signal, which is an indicator of rigidity (or softness) of the sample.
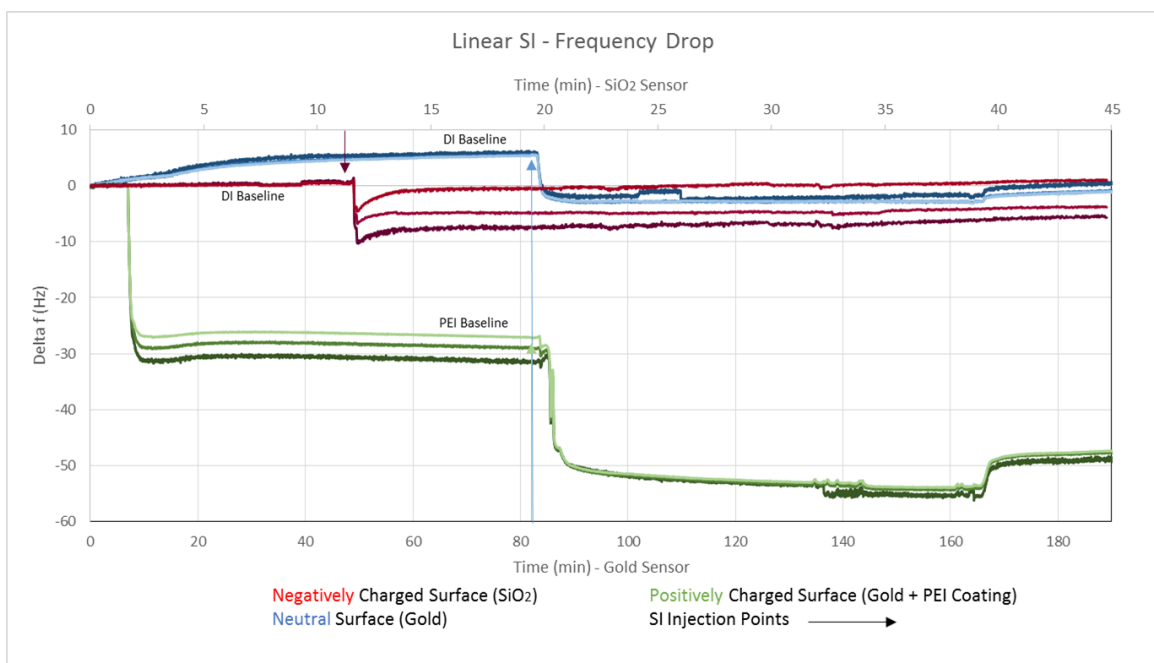
Figure 19: QCM-D Frequency Drop Data - Linear Scale Inhibitor

The red lines in Figure 19 represent linear scale inhibitor interacting with the SiO$_2$ sensor. The DI water baseline from time 0 to ~12 minutes is stable, and hovers around zero. When linear SI is injected at around 12 minutes, the frequency signal drops and stabilizes within ~3 Hz. This is an extremely small frequency change, and can

51

possibly be attributed to the change in relative densities between DI water and the SI solution. There is little evidence to suggest any interaction between the linear scale inhibitor and the negatively charged sensor.

The blue lines in Figure 19 represent the linear scale inhibitor interacting with the gold sensor. The DI baseline is stable at time 80 min. It should be noted that the drift upward to frequency is not indicative of meaningful results, but rather an artifact of the equipment and experiment. At the injection point at time 82 minutes, the frequency drop is ~10 Hz, and all signals are overlapping. This indicative of the linear SI behaving as a rigid film, and shows a small amount of mass adsorbing to the sensor surface.

The green lines in Figure 19 represent the linear scale inhibitor interacting with the gold + PEI sensor. The DI baseline is stable at time 5 min, and the PEI baseline is stable up to time 80 min. At time ~82 min, linear scale inhibitor is injected into the chamber. The magnitude of the frequency drop is ~25 Hz. This is indicative of greater interaction of linear scale inhibitor with the positively charged surface. The signals are also overlapping, indicating that the linear SI behaves as a rigid film.
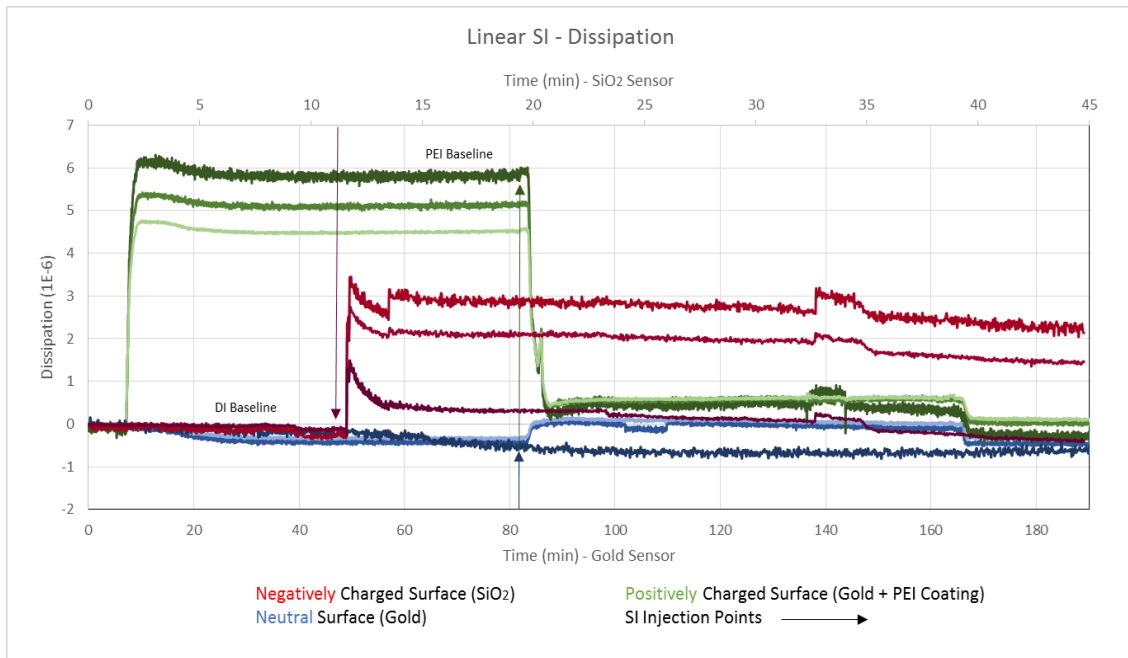
Figure 20: QCM-D Dissipation Data - Linear Scale Inhibitor

The dissipation data for the linear scale inhibitor can be seen in Figure 20. Again, the red lines represent linear SI interacting with SiO_2. Given that the frequency drop response indicates little interaction of SI with the surface, the dissipation data cannot conclusively be attributed to interaction. It is theorized that the particles merely bounce on the surface, and little adsorption is observed.

The blue lines in Figure 20 represent the linear SI interacting with the gold sensor. Two of the signal responses are overlapping, constant, and small in magnitude. This is an indication of rigid-film behavior. The signal for the 9th harmonic drifted into the negative dissipation region. This signal is ignored as a negative dissipation signal is physically impossible.

The green lines in Figure 20 represent the linear SI interacting with the gold + PEI sensor. As observed for the gold only condition, the signals are flat, overlapping, and small in magnitude. This is an indicator for rigid film behavior for linear SI.
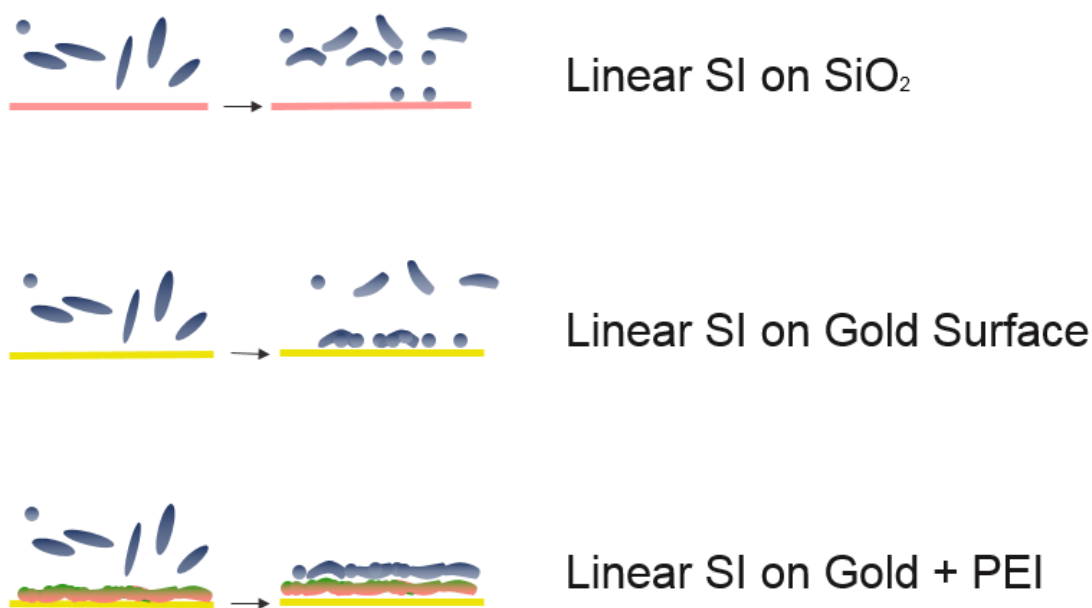
Figure 21: Linear Scale Inhibitor - Surface Model Illustrations

A graphical representation of these interactions can be seen in Figure 21. The PEI particles used were branched chains with positive surface charge, and are represented as tangled masses in Figure 21. As can be seen from Figure 19 and Figure 20, the evidence suggests that there is little to no interaction between linear SI and silicon dioxide. There is evidence of moderate interactions between linear SI and gold,

and there is strong evidence of interaction between linear SI and the gold + PEI surface. It should be noted that the relative difference in size between the linear SI and the PEI particles is dramatic.

We next examine the interactions of the cross-linked scale inhibitor across all three conditions. The frequency drop data for the cross-linked scale inhibitor can be seen in Figure 19. There are three curves shown in this visualization for each condition. Each of these curves corresponds to the 5th, 7th, and 9th harmonics. These harmonics were chosen because they had the cleanest response signals, and they adequately represent the spread in the signal, which is an indicator of rigidity (or softness) of the sample.
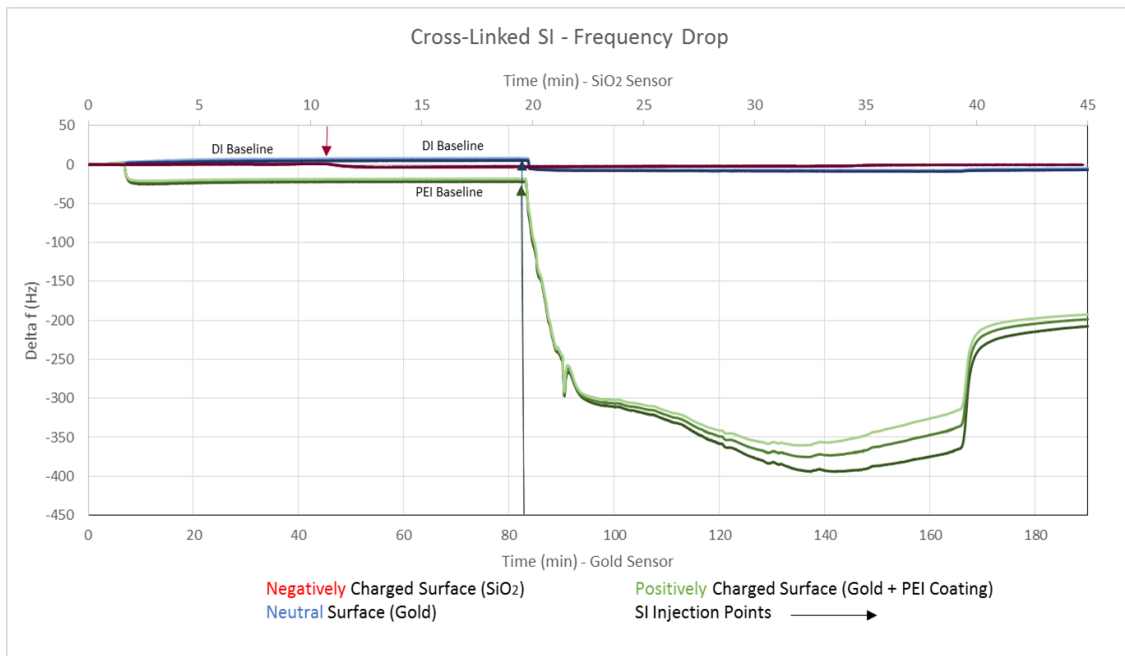
Figure 22: QCM-D Frequency Drop Data - Cross-Linked Scale Inhibitor

The red lines in Figure 22 represent the NSI interacting with the SiO_2 sensor, the blue lines represent the NSI interacting with the gold sensor, and the green lines represent the NSI interacting with the gold + PEI sensor. As can be seen in the figure, the interactions for both the negatively charged and neutral conditions are minimal. They are on the order of ~10 Hz frequency drop. For the positively charged condition, there is a frequency drop on the order of ~400 Hz. This is an indication of a comparatively large amount of mass adsorbing to the surface.

Between the injection point (~82 minutes) and the DI water post-flush point (~165 min), the signals are relatively overlapped, with deviation between the curves as time progressed. A possible explanation for this behavior is due to the fact that the NSI solution is an unstable colloidal system. The zeta potential of the scale inhibitor is on the order of -15 mV. At 45° C, it is possible for thermal energy to overcome the repulsive electrostatic force between particles and observe Van Der Waals interactions. The changing frequency signal can thereby be changing with time due to these forces causing agglomeration of particles.
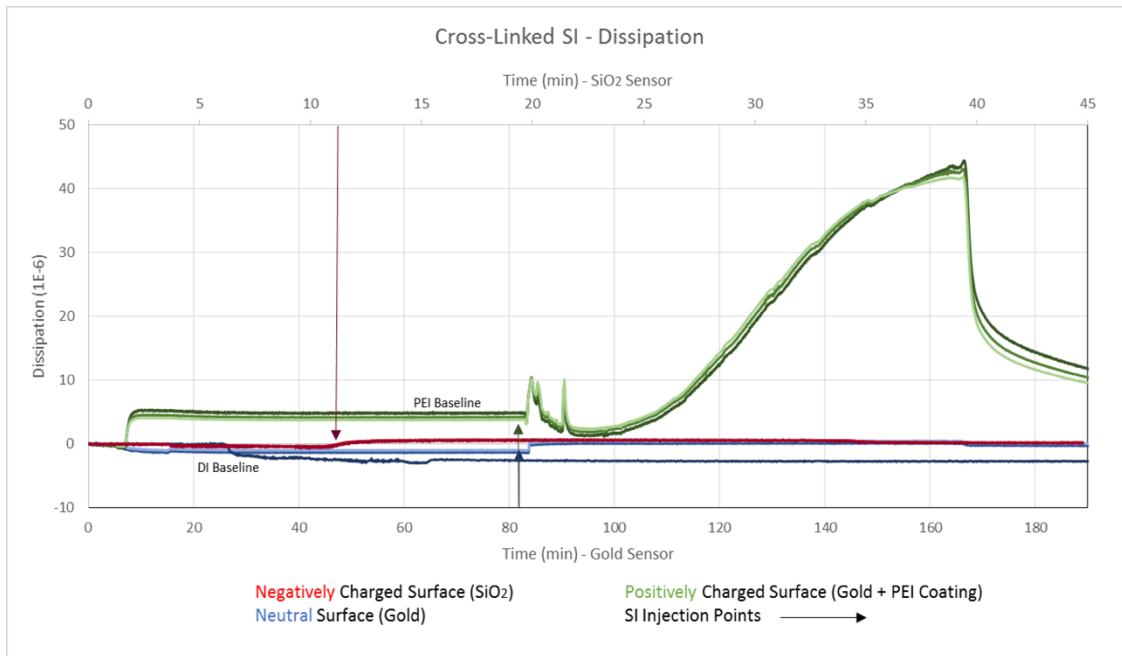
Figure 23: QCM-D Dissipation Data - Cross-Linked Scale Inhibitor

The dissipation data for the cross-linked scale inhibitor can be seen in Figure 23. As before, the red, blue, and green lines correspond to the negative, neutral, and positively charged surface conditions. The dissipation signals for the negative and neutral conditions are small in magnitude and overlapping. The dissipation signal for the positively charged conditions are large, and changing over time. These are very strong indicators that our NSI systems behaves as a viscoelastic particle.
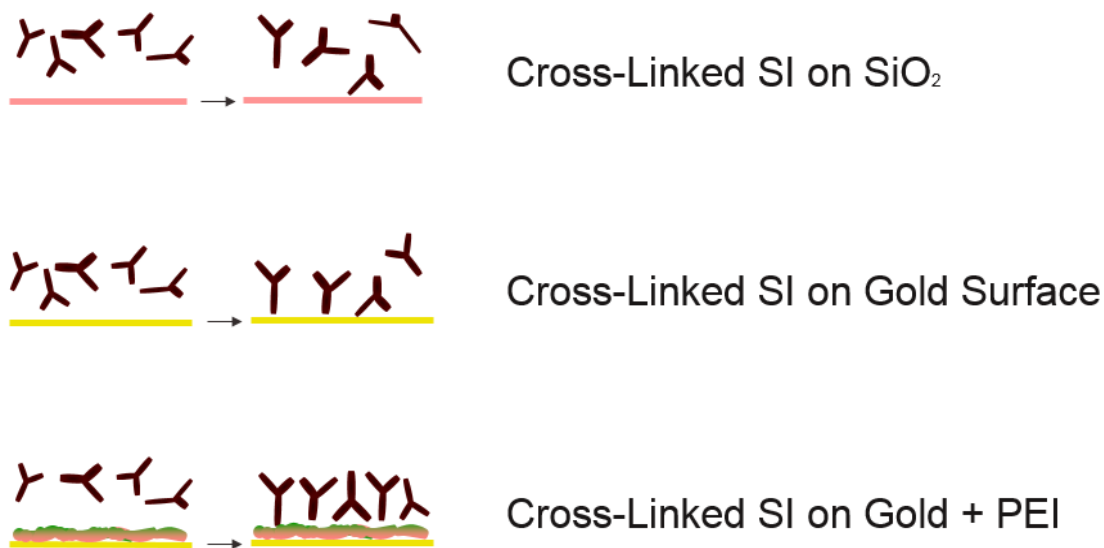
Figure 24: Cross-Linked Scale Inhibitor - Surface Model Illustrations

A graphical representation of these interactions can be seen in Figure 24. The PEI particles used were branched chains with positive surface charge, and are represented as tangled masses. Although not to scale, the relative sizes between PEI and the NSI can be seen in the figure. The evidence suggests that there is little to no interaction between cross-linked SI and silicon dioxide. There is evidence of moderate interactions between cross-linked SI and gold, and there is strong evidence of interaction between cross-linked SI and the gold + PEI surface.

Finally, we would like to gain an idea of how our cross-linked scale inhibitor behaves in comparison to our linear scale inhibitor. In Figure 25 and Figure 26 we can compare the adsorption behavior of linear and cross-linked scale inhibitor for both the negatively charged and positively charged surfaces. In Figure 25, we can see that despite

the magnitude of the frequency drop being small, there is evidence of more mass

adsorbing to the silicon dioxide sensor surface. In Figure 26, we can see that there is a

significant difference between linear SI adsorption and NSI adsorption to a positively

charged surface.
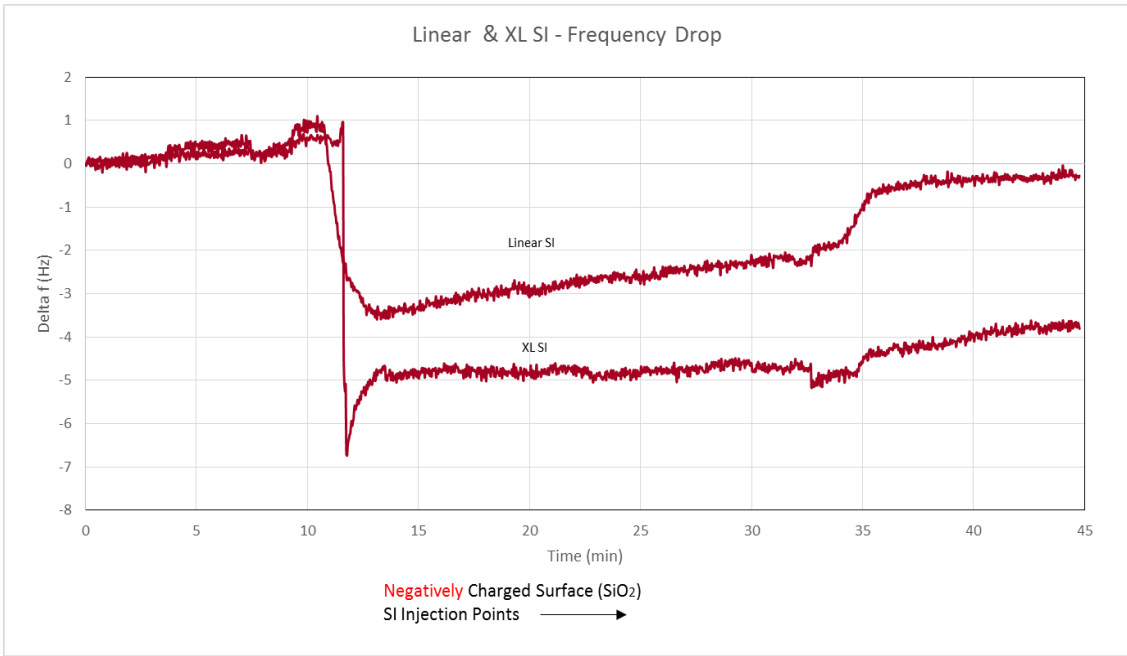
Figure 25: Frequency Drop Data (5th harmonic) - Negatively Charged Surface
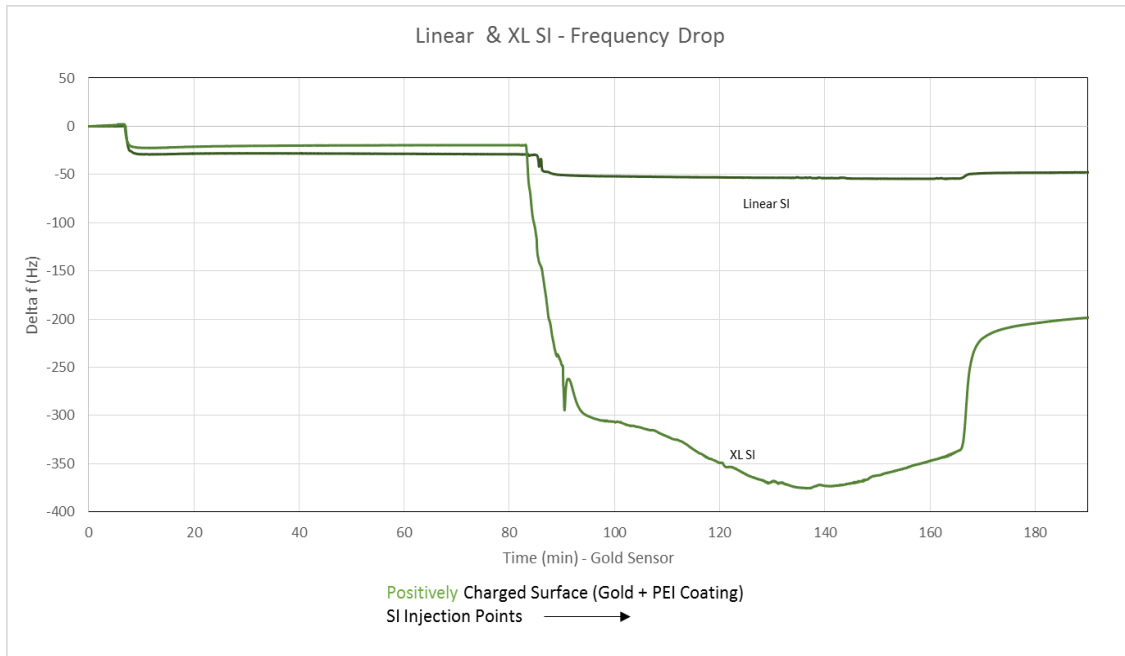
Figure 26: Frequency Drop Data (5th harmonic) - Positively Charged Surface

4.4 QCM-D Conclusions Summary

Even with a qualitative analysis we can glean a significant amount of information from these QCM-D data. Based on the data presented previously we can conclude the following:

1. Both linear and cross-linked scale inhibitor display little-to-no electrostatic interaction with negatively charged surfaces. Therefore, we can say that any retention observed in further sandpack experiments (using quartz sand) can be attributed to mechanical retention in pore space.

2. Linear scale inhibitor behaves as a rigid film when adsorbing to neutral or positively charged surfaces. That is, there is evidence of tight packing under these conditions due to electrostatic interactions.

3. Cross-linked scale inhibitor behaves as a viscoelastic film when adsorbing to neutral or positively charged surfaces.

4. Cross-linked scale inhibitor has a greater adsorption to neutral and positive surfaces than the linear scale inhibitor.

5. DYNAMIC RETENTION STUDIES

5.1 Objective

Sand pack experiments are performed to evaluate the behavior of scale inhibitor in an analog of a reservoir environment. The design of the experiment is such that we simulate conditions in the reservoir rock before, during, and after injection of scale inhibitor.

5.2 Materials and Methods

A glass chromatography column was chosen as the primary vessel for the sand pack for several reasons: relatively low cost of materials, ease of assembly and preparation, and speed of experimentation. The glass chromatography column also contains an outer sleeve through which water can flow. This enables us to set and control the temperature at 45 $^\circ$C throughout our experiments.

Quartz sand is used exclusively in these experiments. Quartz is a mineral composed of silicon and oxygen atoms in a continuous framework of SiO_4 silicon-oxygen tetrahedral. The chemical formula for the mineral is SiO_2. The samples used in these experiments were provided as an industry sample for academic research. The grade is F-75, and the size used is 100 mesh (~150 microns). When packed into a cylinder for experiments, this sand typically yields a porosity of ~35% and permeability in the 8-10 Darcy range. The assembled and filled sandpack column can be seen in Figure 27.

Figure 27: Sandpack Glass Chromatography Column, PTFE Endcaps, Nylotube, and Swagelok Three-Way Valves

Sandpack Column Preparation Procedure

1. Acquire 200 mesh steel. Cut four circular sheets such that two layers fit exactly in the PTFE fittings in the endcaps flush against the NPT-Swagelok fitting adapter. The desire is that the two 200 mesh layers prevent sand migration into tubing, which could form unwanted blockages.

2. Assemble 2 endcaps with screw cap, NPT fitting, Nylotube, ferrules and caps, O-rings, and Swagelok three-way valves. Use medium density Teflon tape on PTFE fittings (one layer). Lower density Teflon tape will require more layers on the threads.

3. Screw endcap assemblies on the top and bottom ends. Attach a vacuum gauge to the bottom end. Pull a vacuum on the empty column to ensure no leaks for ~1 min.

    i. If a leak is detected, apply positive gas pressure (~5 psi) and use soapy water to detect location of leak. Adjust endcaps as necessary. Use appropriate safety measures under positive pressure.

4. Once column is cleared of leaks, weigh the assembled column and record the mass.

5. Prepare ~130 g of quartz sand and a funnel to place on the top of the column.

6. Remove top endcap assembly. Clamp the column vertically onto a vibration table. Place the funnel on top of column, and pour a small amount of sand (~2 g) into the column. Use a rubber mallet to tap the column and settle the sand at the bottom of the column. Ensure that no sand has fallen passed the two 200 mesh layers. If so, disassemble the column and start over from Step 1.

7. Turn on the vibration unit, and begin pouring the remaining ~100 g of sand into the funnel.

8. Once the sand level has reached near the top, use a caliper (or some other tool) to measure the exact depth of the NPT fitting into the screw cap assembly. By hand, fill with sand to this exact level. Be sure to use the rubber mallet to tap the column and ensure even/homogenous spreading of the sand.

9. Once the desired level has been reached, used a needle and metal rod to tamp down two layers of 200 mesh steel to the surface. Screw down the NPT fitting

into the screw cap, and attach the Nylotube and Swagelok valve. (If necessary, be sure to re-apply Teflon tape to the NPT threads.)

10. Attach a vacuum gauge to the bottom end. Pull a vacuum on the empty column to ensure no leaks with air for ~10 min.

    i.   If a leak is detected, apply positive gas pressure (~5 psi) and use soapy water to detect location of leak. Adjust endcaps as necessary. Be sure to clean all fluids from column before removing positive pressure. If fluids enter the column, disassemble the column and start over from Step 1.

11. Once column is cleared of leaks, weigh the assembled and filled column. Record the mass.

12. Prepare model brine solutions for anion[4]. Exact mixture components can be seen in Table 4. For saturation, do not add $NaHCO_3$.

13. Pull a vacuum on the column from the top end, and use negative pressure to pull anion solution from the bottom end of the column.

14. Weigh the saturated column and record the mass.

<center>Column Characterization Procedure – Permeability Test</center>

1. Prepare model anion[5]. Exact mixture components can be seen in Table 4. For characterization, do not add $NaHCO_3$.

[4, 5] Model anion is prepared beforehand without sodium bicarbonate due to its natural tendency to break down over time in solution. Sodium bicarbonate is only added on the day of use.

<center>65</center>

2. Using the dimensions of the sand pack, note the length of the pack, and the effective diameter. The effective diameter is the weighted average of diameters across the column. The weighting factor is the fractional length.

$$D_{eff} = \sum \left(\frac{l_n}{l_{tot}}\right)(D_n)$$

3. Connect the column to the inlet and outlet Nylotube lines. Connect the pressure transducers to the inlet and outlet lines. The assembly used can be seen in Figure 28.
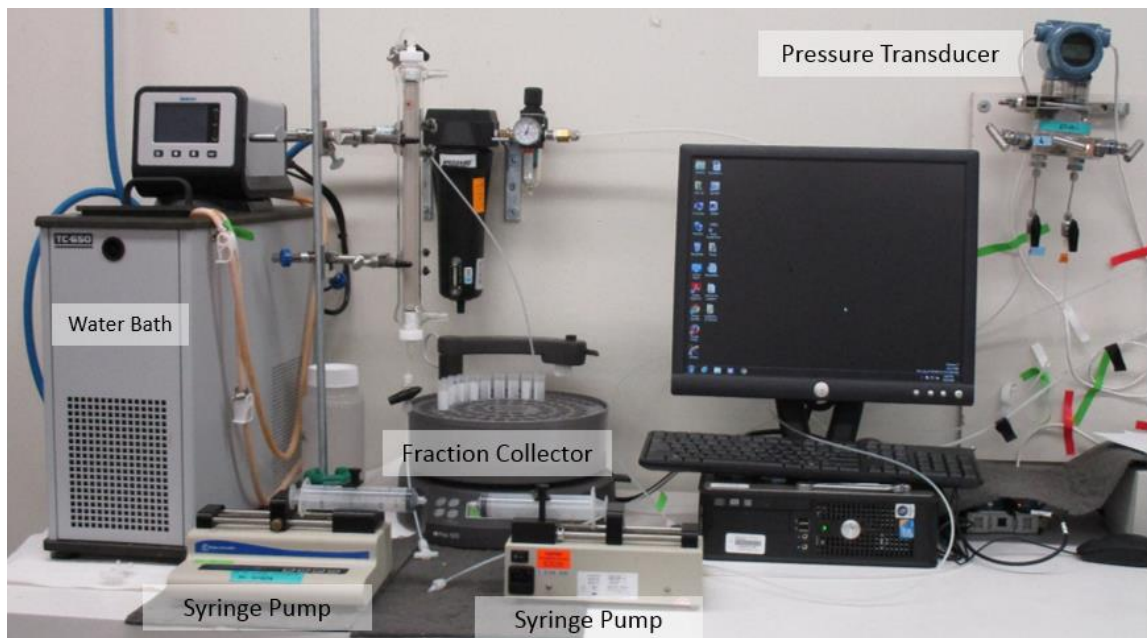
Figure 28: Dynamic Retention Experimental Setup

4. Use the pumps and DI water to purge the transducer and transducer lines of any air bubbles. Be sure to use an adequate flow rate (>10 mL/min).

5. Close off the transducer lines with an in-line Swagelok valve, and purge the injection line with the anionic brine.

6. Begin flowing anionic brine through column while measuring the pressure drop across the column as a function of flow rate. Use Darcy's Law to calculate the permeability of the column. Use several flow rates.

$$k = \frac{q * \mu * L}{A * \Delta P}$$

7. Validate that the correlation coefficient is close to 1. If the data are non-linear, scrap the column and re-pack.

<p align="center">Column Characterization Procedure – Tracer Test</p>

1. Prepare model anion[6]. Exact mixture components can be seen in Table 4. For characterization, do not add $NaHCO_3$.

2. Prepare 1% KCl solution in anionic brine (without $NaHCO_3$).

3. Connect the column to the inlet and outlet Nylotube lines. Connect the pressure transducers to the inlet and outlet lines. The assembly used can be seen in Figure 28.

---

[6] Model anion is prepared beforehand without sodium bicarbonate due to its natural tendency to break down over time in solution. Sodium bicarbonate is only added on the day of use.

4. Use DI water to purge the transducer and transducer lines of any air bubbles. Be sure to use an adequate flow rate (>10 mL/min).

5. Close off the transducer lines with an in-line Swagelok valve, and purge the injection line with the 1% KCl solution.

6. Place 50-70 tubes in fraction collector depending on desired resolution of tracer curve.

    i. Use an adequate fraction size (~0.1 PV ≈ 2 mL). The flow rate was 1 mL/min.

7. Drain the effluent line into waste container. Move effluent line to fraction collector. Program fraction collector according to desired collection volumes.

8. Begin pumping tracer solution through column. As soon as fluid reaches end of effluent line, begin timer on fraction collector.

9. At mid-point, stop pump and pause fraction collector. Drain effluent line into collection tube(s). Change injection fluid to model anion. Purge injection line with model anion.

10. Resume flowing of model anion through column. When fluid reaches the end of the effluent line, resume the timer on the fraction collector.

11. At the end of the collection time, turn off all pumps, and close all valves on the setup.

12. Transfer all samples to cuvettes for UV-Vis analysis.

    i. KCl adsorbs at 300.00 nm wavelength.

13. Prepare various concentrations (0-1% KCl in anionic brine). These will be used for calibration of the UV-Vis analysis for concentration determination of the fractional samples.

14. Use UV-Vis Spectrophotometer to determine concentration as a function of cumulative pore volume injected.

15. Plot the normalized concentration (C/C_{max}) versus Pore Volumes Injected. An ideal curve can be seen in Figure 29.
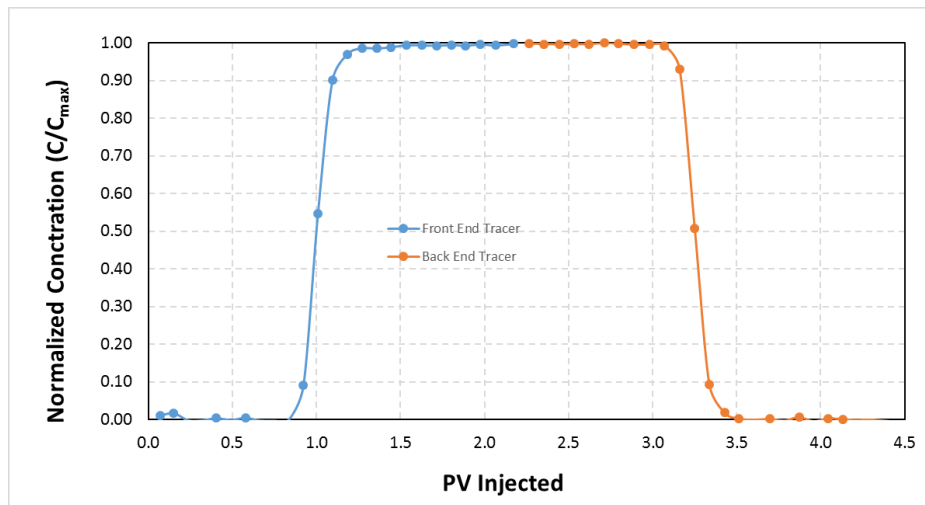
Figure 29: Example of Ideal Tracer Curve for Sandpack

16. The .50 normalized concentration point should correspond to the 1 PV by mass amount. If this value differs from the PV by weight calculation by >10%, discard the column and start over. If the tails drift (and cannot be explained by

69

dispersion), or if the tracer curve is otherwise non-uniform, discard the column and start over. An example of a bad tracer curve can be seen in Figure 30.
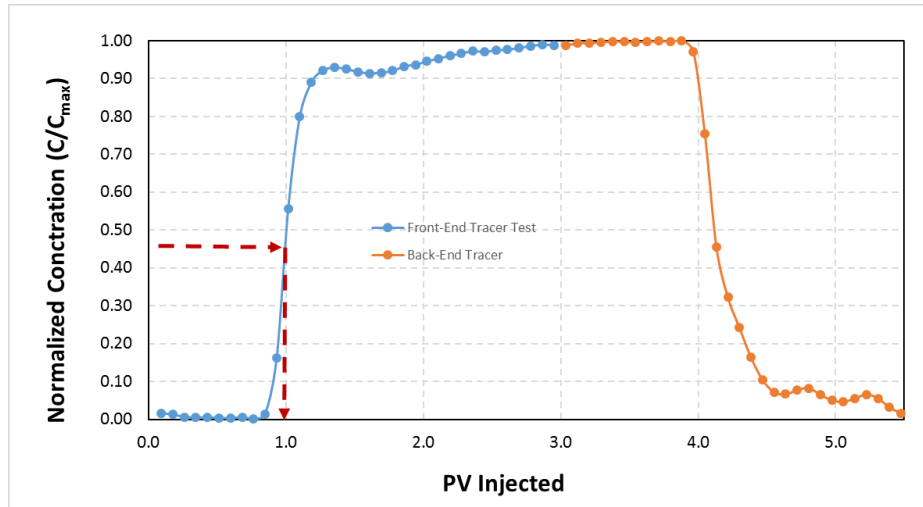
Figure 30: Example of Tracer Curve for Poor Sandpack

Sandpack Flood Procedure

1. Prepare a scale inhibitor solution of desired concentration in model brine according to procedures outlined in the MIC section of this document.

2. One day before the injection, attach rubber hoses from the water bath to the sleeve of the glass column. Set the temperature to 45 °C, begin flowing, and wait overnight for temperature equilibration.

3. Purge transducers and transducer lines with DI water.

4. Close off transducer lines, and purge injection line with NSI solution.

5. Drain effluent line into waste, and then place effluent line in graduated cylinder. Note volumes on injection pump. It is critical to record the injection volume of NSI for later analysis.

6. Inject the NSI solution at 0.4 mL/min (~6 ft/D) for a total of ~3 PV.

7. After the injection, drain the effluent line into the graduated cylinder and verify total injection volume. Save fluid for TN analysis.

8. Shut-in overnight.

9. Set up dual injection (T-joint) for anion and cation. Prepare full anion solution.

10. Prepare 40-50 tubes in fraction collector. Adjust fraction volumes for appropriate resolution ~0.2 PV per fraction).

    i.   These experiments used 4 mL collection volumes for each tube.

    ii. Program fraction collector accordingly.

11. Inject both brine solutions at a total flow rate of 0.2 mL/min. When fluid has reached end of effluent line, begin timer on fraction collector.

12. Flush in forward direction for ~3 PV. At this point, stop all pumps, close all valves, switch the injection and effluent lines, and resume fluid injection in the reverse direction. Continue collecting fractional samples. If the pressure drop across the column is less in the reverse direction, there is evidence of a filter cake on the inlet side. Further evidence of a filter cake will appear in TOC-TN measurement.

13. After a total of ~6 PV have been injection (3 PV forward and 3 PV reverse), end the flood.

<center>Scale Inhibitor Retention Measurement – TN Procedure</center>

1. Collect all samples from sandpack flood. Prepare TOC-TN sample vials and caps.

2. Dilute the fraction samples so that the total brine content is under 4000 ppm. This is to preserve the TOC-TN instrument. Record the dilution factor for each sample.

3. Prepare calibration curve using KNO_3 as TN standard. The calibration curve should contain at least 5 points. Auto-dilution on the TOC-TN instrument can be used.

4. Analyze the TN content of the pre-injection SI fluid, the post-injection effluent (collected in the graduated cylinder), and back-calculate the SI concentration of each sample using the appropriate dilution factors and ratio of N: SI in the synthesized batch. These concentrations can be used to calculate the amount of scale inhibitor retained in the sand pack via mass balance. That is, the initial mass of scale inhibitor corresponds to the mass of retained scale inhibitor. Subtracting the fractional amounts of scale inhibitor flushed out corresponds to the retention as a function of throughput.

$$m_{SI,Initial} = ([SI]_{Pre-Injection} * V_{Pre-Injection}) - ([SI]_{Post-Injection} * V_{Post-Injection})$$

$$m_{SI,\ T=n} = m_{SI,Initial} - \sum [SI]_n * V_n$$

<center>72</center>

$$Retention_{T=n} = \frac{m_{SI,\ T=n}}{m_{Sand}}$$

5. The retention can be measured on an absolute (mg SI / g sand) or on a percentage value. For the percentage calculation the $(m_{SI,Initial}/m_{Sand})$ value is used as the 100% point. Using these calculations, retention curves can be generated such as those below.

Percentage Retention
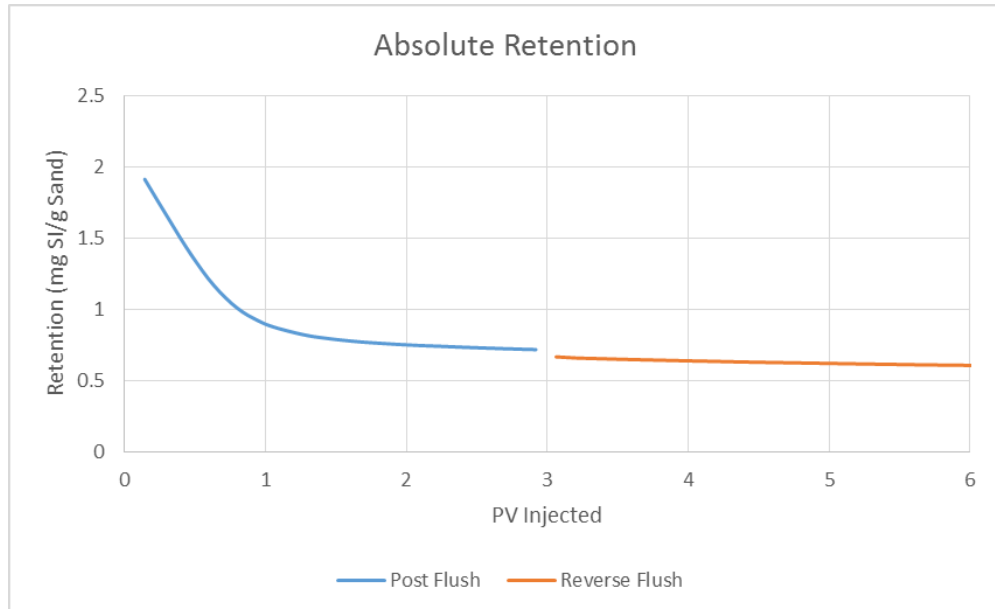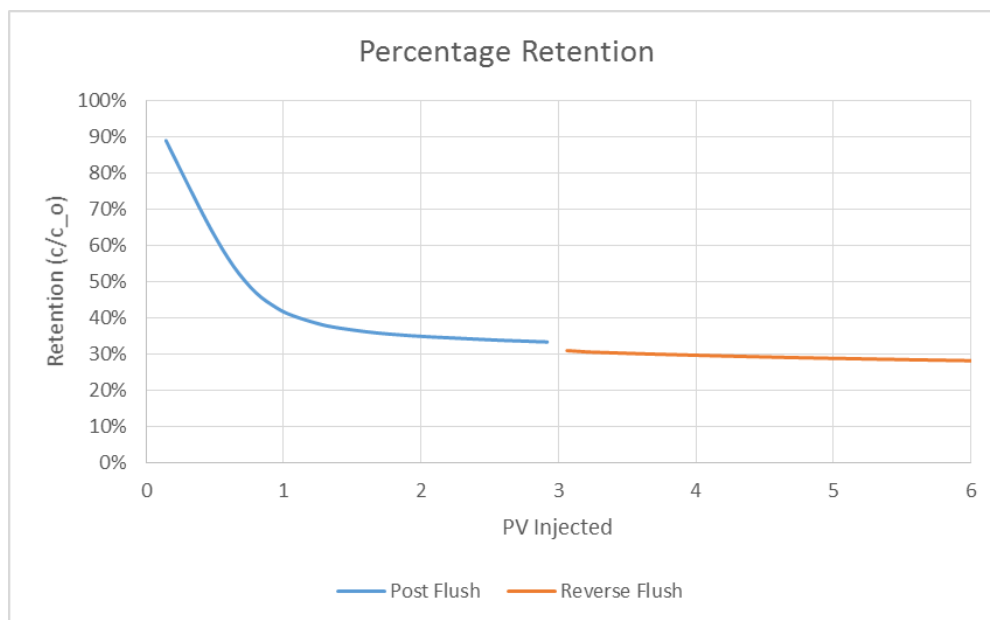
Experimental Equipment

A Cary 60 UV-Vis Spectrophotometer made by Agilent Technologies was used to measure the turbidity (i.e. absorbance) of each sample. The instrument can be seen in Figure 9.

Particle size and zeta potential measurements were done using a NanoBrook Omni particle sizer and zeta potential analyzer manufactured by Brookhaven Instruments Corporation. The instrument can be seen in Figure 10.

A Quizix QX500 Series pump (Figure 31) was used for characterization of the columns. The pump is capable of constant rate and constant pressure delivery and thereby well suited for characterization of columns.

Figure 31: Quizix QX 500 Pump (Chandler_Engineering, 2017)

Teledyne Isco pumps were also used throughout these experiments. Two Teledyne 500D Syringe pumps were used for dual injection of the incompatible brine mixtures. This allowed for the two brines to mix just as they were entering the column via a T-joint.

Figure 32: Teledyne Isco 500D Syringe Pump (Teledyne, 2017)

A Shimadzu Total Organic Carbon Analyzer with Test Method for Total

Nitrogen (TOC-L with TNM) was used as the analytical tool for measuring the amount

of scale inhibitor in solution. The analysis in this section relies on the detection of

nitrogen in solution, and the instrument setup can be seen in Figure 33. The analytical

method can measure total nitrogen (TN) from 0.2 – 500 mg/L with concentrations up to

10,000 mg/L possible by sample dilution. The method detection limit is $\leq .05$ mg/L TN.

Figure 33: Shimadzu TOC-L Analyzer and ANSI Auto-Sampler

TOC analyzers can measure total carbon (TC), total organic carbon (TOC), inorganic carbon (IC), non-purgeable organic carbon (NPO), and total nitrogen (TN). The measurement involves oxidizing organic molecules in a sample, detecting and quantifying the oxidized elements, and presenting the results of mass per volume of sample. The unit obtains this information by sampling specific volumes of fluids, adding a small percentage of acid (~3%) to remove salts, sparging the fluid with compressed air gas, injecting the fluids into a combustion chamber with platinum catalytic beads, combusting at 680 ºC, and ejecting the gases through a nondispersive infrared sensor

(NDIR) for peak detection. The area under the detection peak is then correlated to a concentration of a specific element in solution.

5.3 Results and Discussion

A number of sandpack experiments were performed in order to investigate the effect of particle size and concentration on retention. A summary of sandpack experiment conditions can be seen in Table 11.

Table 11: Summary of Dynamic Retention Experiment Column Conditions

Sand Pack #	SI Concentration (ppm)	Solvent	SI Type	Particle Size (nm)	Zeta Potential (mV)
1	1,000	Synthetic Seawater	Cross-Linked	1200	-21.18
2	1,000	Model Brine	Cross-Linked	1100	-20.27
3	4,000	Model Brine	Cross-Linked	900	-28.63
5	10,000	Model Brine	Cross-Linked	1100	-21.71
6	10,000	Model Brine	Cross-Linked	400	-24.16
7	10,000	Model Brine	Cross-Linked	700	-8.40
8	10,000	Model Brine	Cross-Linked	280	-20.14
9	1,000	Model Brine	Cross-Linked	400	-14.72
10	1,000	Model Brine	Linear	-	-15.98
11	10,000	Model Brine	Linear	-	-11.30

A complete graphical representation of all sand pack experiments can be seen in Figure 34. This view represents that absolute retention (mg SI/g Sand) vs throughput (PV). The most noticeable result of these experiments is the relationship between scale inhibitor concentration and initial retention. Note that every experiment had the same volume (~3 PV) of SI injected into the sandpack. As the concentration of the injected fluid increases, the initial retention increases. The 10k ppm SI trials had initial retention of 6-8 times greater than the 1k ppm experiments.

The sharp drop in retention in the curve(s) at the 3 PV point indicates the presence of a minor filter cake on the inlet of the column. A filter cake is the plugging of SI at the front end of the column. The filter cake appeared to be present in columns with larger average particle sizes. However, the filter cake was not always evident in the data, and the drop is minor in the observed data.
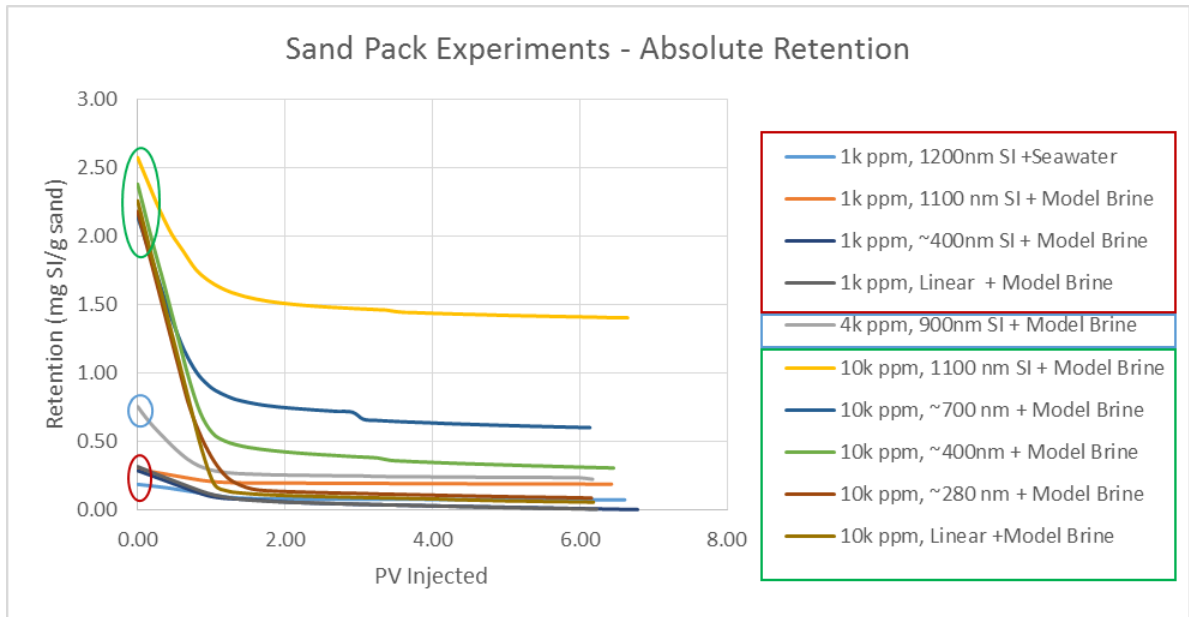
Figure 34: Sand Pack Experiments – Absolute Retention

If we examine the data for the 1k ppm SI experiments, we can observe the trend of particle size versus throughput. This can be seen in Figure 35. The top two curves represent the largest of particle sizes injected. However, the two brines used in these experiments are different: one was performed in synthetic seawater, and the other was performed in the model brine. The synthetic seawater trial was performed initially because of the lack of scale precipitation due to brine incompatibility. Once the first trial proved successful, the model brine was introduced into the system. The difference in absolute retention between these two curves can be attributed to the difference in particle size and charge in different brine solutions.
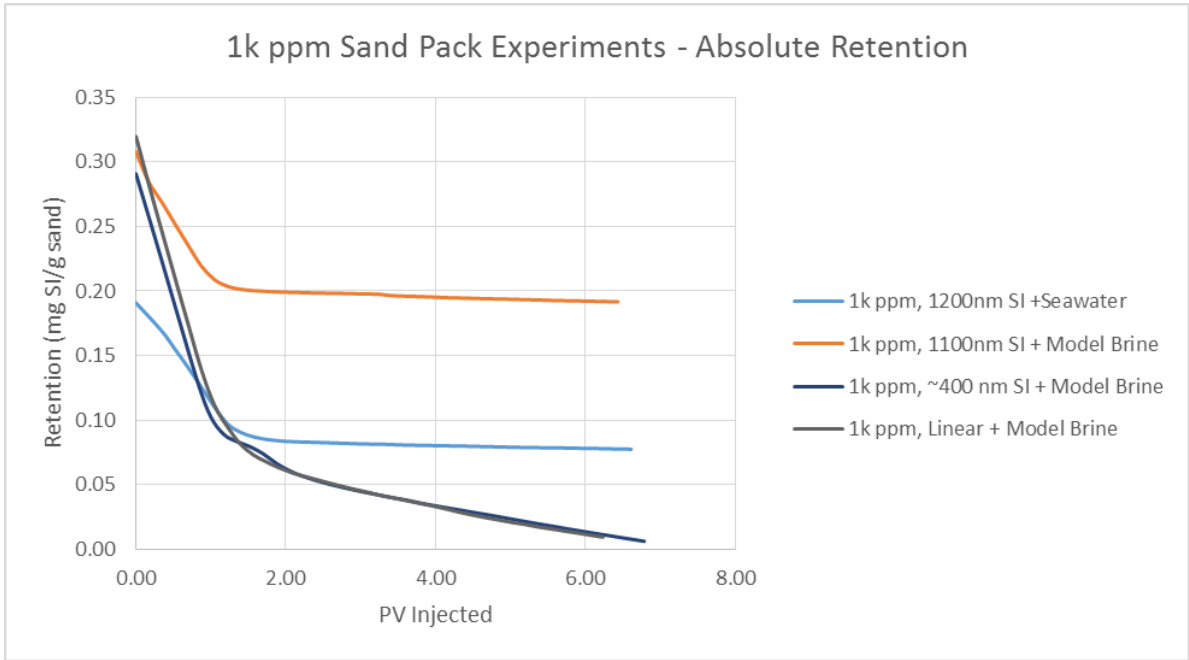
Figure 35: Absolute Retention – 1,000 ppm SI Experiments
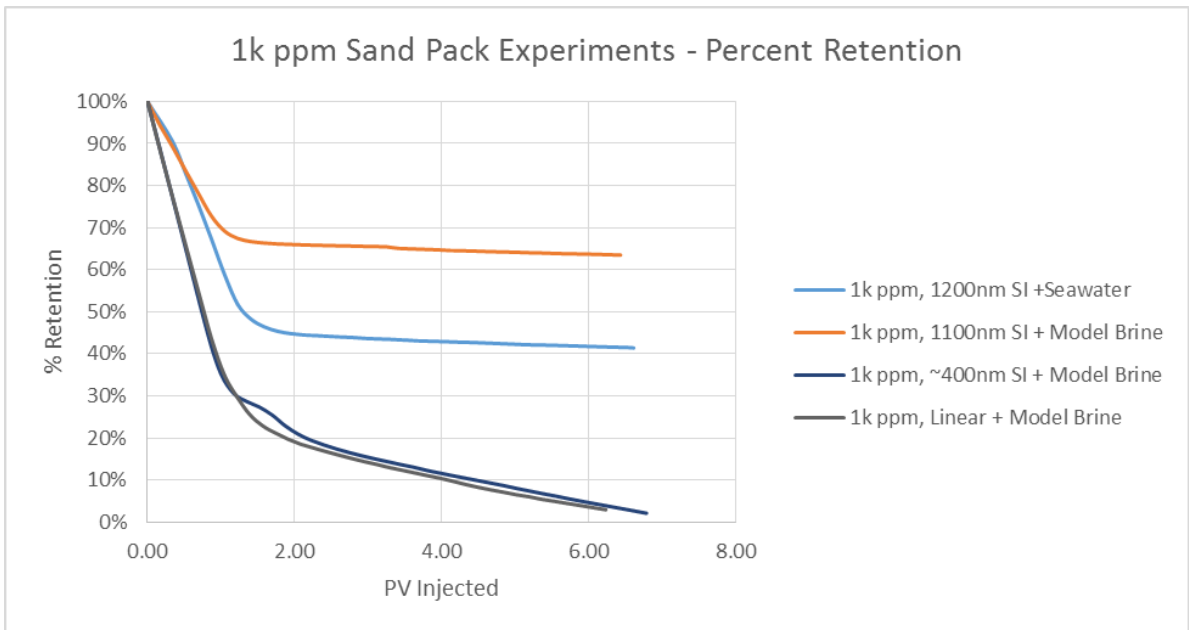
Figure 36: Percent Retention - 1,000 ppm SI Experiments

81

What is most significant here, however, is that we see at ~400 nm particle size in model brine, we observe retention behavior similar to that of the linear SI solution. This is evidence that we have a lower bound on successful scale inhibition when our particle size is greater than 400 nm. A similar trend is seen when we look at the percentage retention (Figure 36).

Using the bundle of tubes model, we can approximate the throat size by:

$$d = \sqrt{\frac{k * 96}{\phi}} = \sqrt{\frac{(9.87 * 10^{-12} \ m^2)(96)}{.35}} = {\sim}50 \ \mu m$$

Where d is the pore throat diameter, k is the permeability (m^2), and ϕ is the porosity (percentage) (Jurgawczynski, 2007). This calculation is merely an approximation based on rough in-situ permeability measurements (1 D = $9.8*10^{-12} \ m^2$) and porosity measurements. From the above calculations and experimental results, we can see that a particle size: pore throat size ratio of > .008 is required to observe retention.

As we can see for the 1,000 ppm SI experiments, our maximum percent retention curve yields a result of 65% retention (0.19 mg SI/g Sand). This result is much greater than the linear SI trial, which yielded ~3% (0.009 mg SI/g Sand).

We can now examine the data for the 10,000 ppm SI sandpack experiments. The absolute retention and percent retention for this series of experiments can be seen in Figure 37 and Figure 38, respectively.
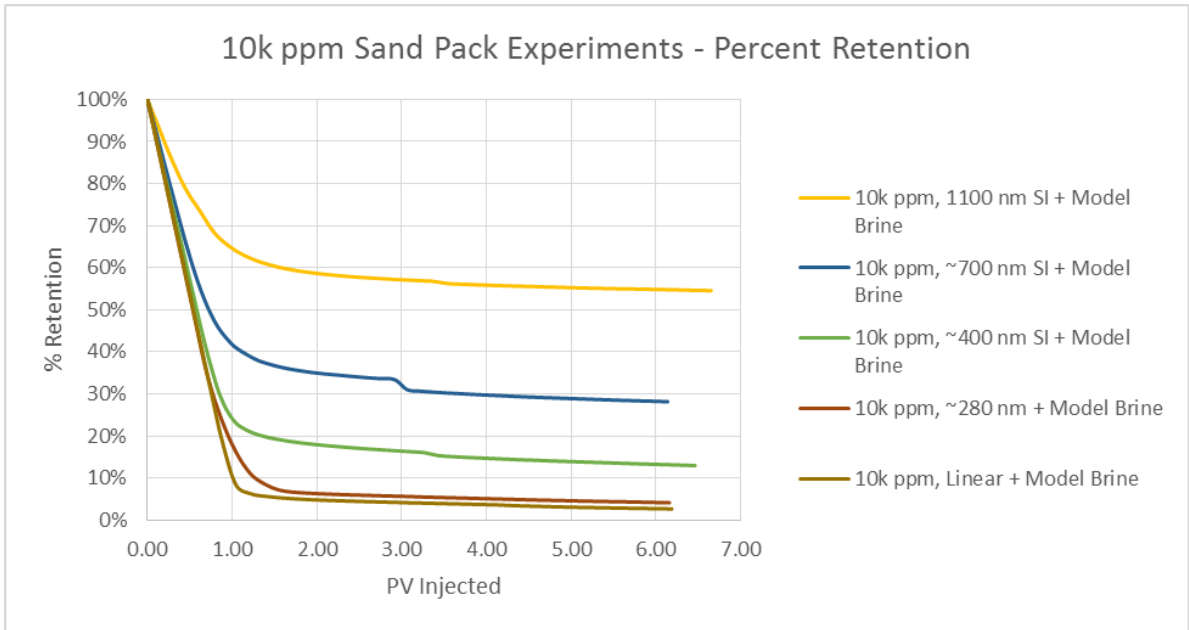
Figure 37: Absolute Retention - 10,000 ppm SI Experiments
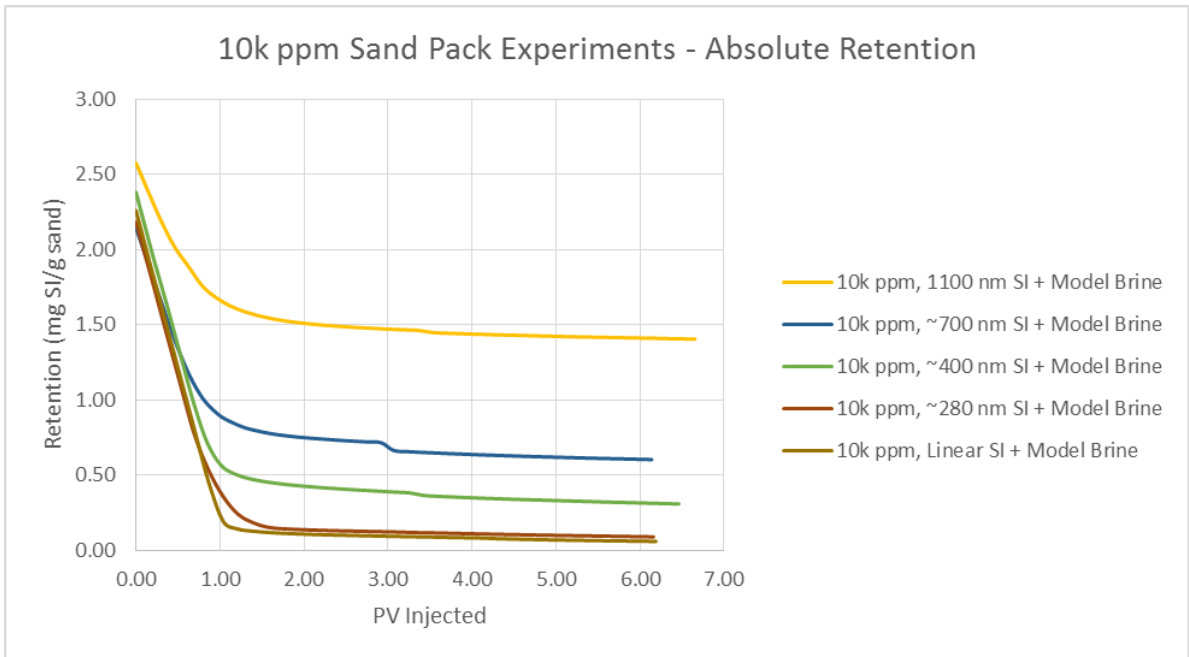
Figure 38: Percent Retention - 10,000 ppm SI Experiments

83

Retention vs throughput for 10,000 ppm SI is largely a function of particle size. As we decrease the particle size, we can see that the retention values gradually fall closer to that of the linear SI retention curve. Our lower bound for this case appears to be ~300 nm particle size, whereas previously for 1000 ppm SI our lower bound was ~400 nm. We can see moderate evidence of filter cake for the ~700 nm and ~400 nm trials. When looking at the percentage retention chart, we can see that our maximum percent retention is on the order of 55% after 6 PV of throughput (1.48 mg SI/g Sand). This is exceptionally greater than the linear SI trial, which yielded ~3% (.06 mg SI/g Sand).

5.4 Dynamic Sandpack Experiments Conclusions Summary

These dynamic sand pack experiments were performed as a proof-of-concept assay for our scale inhibitor system. From our data we can conclude the following:

1. Initial values for retention are largely governed by the scale inhibitor concentration in the injection fluid. Higher initial concentrations leads to higher initial absolute retention values.

2. The retention values versus throughput are largely governed by the particle size of the scale inhibitor. Larger particle size lead to higher percent retention over time.

3. For both low and high concentrations of scale inhibitor, our NSI has much higher retention than the linear scale inhibitor alone. Greater retention will lead to longer treatment lifetimes due to mechanical pore plugging. Hydrolysis of the cross-linker will lead to sustained release of scale inhibitor over time.

4. In conjunction with the QCM-D results, we can conclude that retention in our system is mostly due to mechanical means rather than electrostatic adsorption to the rock surface.

6. PROJECT CONCLUSIONS

6.1 Summary of Results

The initial objectives of the project were to firstly develop a repeatable synthesis recipe for a nanoized scale inhibitor with adequate brine compatibility, with a sufficient delayed-release profile, and with enhanced retention over current commercial products. A continuing objective is to establish that our system has an extended treatment lifetime under anaerobic conditions and at high temperatures (~95 ºC).

Our NSI composition consists of a ratio of sulfonate functional groups to scale inhibitor monomers, AMPS: (SA/AA). Our synthesis and brine compatibility results found that ratios greater than 15mol% AMPS NSI (i.e. AMPS content is 15mol% of all monomers) show sufficient brine compatibility. Our experiments focused on maximizing the scale inhibitor components in the NSI whilst maintaining an adequate brine compatibility. That is, we aim to ensure that no pseudoscale is formed when we inject our NSI into the formation. Therefore, we posit that our 20mol% AMPS recipe is the ideal choice for this project.

The studies of the MIC over time showed the release profile of the various recipes. The results of these experiments have shown that our NSI system can sustain release of scale inhibitor of durations up to 40 days in a static environment.

Dynamic retention studies (squeeze treatment simulations) using our NSI yielded retention results between 20 - 60% after 6 PV of throughput (depending primarily on particle size). Using a 10,000 ppm NSI solution yielded retention between 0.4 - 1.4 mg SI/ g Sand. For comparison, previous experiments using commercial cross-linked scale

inhibitors (AlOOH-SPCA) yielded retention results of 60% after 3 PV, but dropped to less than 1% of total injected scale inhibitors after 6 PV of throughput (Yan C. , et al., 2013).

Our system can be tailored specifically to fit the needs of the reservoir, as the process involves synthesizing a gel and mechanically creating a nanoparticle in solution. Using a blender, we can control the particle size depending on the speed of blending (shear rate) and the time duration exposed to shear.

6.2 Primary Obstacles

By far the biggest difficulty in experimentation is attributed to controlling the particle size. The procedure followed herein utilized a commercial blender. It is difficult if not impossible to maintain a constant shear rate with a countertop appliance. When measuring particle size via dynamic light scattering (DLS) bimodal, or even trimodal distributions in some instances, were obtained. It would be recommended to determine a more consistent manner of breaking the gel into solution before pursuing field application. Possible methods to homogenize the solutions are to utilize ultra-sonication of the scale inhibitor solution or to use a shear-history simulator to break the gel.

6.3 Recommendations for Future Work

An additional objective of this project is to improve upon the overall treatment lifetime scale inhibitor treatments. Based on the MIC investigations, we have evidence of sustained release up to 40 days. However, to further bolster our results, dynamic retention/squeeze treatment experiments should be performed under anaerobic conditions at temperatures ~95 $^\circ$C.

The setup will include a steel sandpack column rather than glass. Additionally, the heating element will be electrical, including a metallic component wrapped around the steel column. Insulation will cover the outside and prevent heat loss. After characterization of the column (permeability, tracer test), the column will be purged with anionic brine under anaerobic conditions. All fluids used subsequently will be prepared under anaerobic conditions. The model brine post flush will continue for up to 100 PV of throughput, and evidence of the final treatment lifetime will be evident based on a pressure spike measured across the column. The pressure spike will indicate that all scale inhibitor has been released, and scale formation from the incompatible brine mixtures will begin to plug available pore space.

REFERENCES

Baugh, T. D., Lee, J.-Y., & Winters, K. (2012). A Fast in Information-Rich Method for Scale Inhibitor Performance. *Offshore Technology Conference*.

Bonnett, N., Fieler, E., & Hen, J. (1991). Application of a Novel Squeeze Scale Inhibitor in the Beryl Field. *Society of Petroleum Engineers*, *23107.*

Carrell, C. (1987). The Occurence, Prevention and Treatment of Sulphate Scale in Shell Expro. *Offshore Europe 87.* Aberdeen.

Carrell, K. D. (1987). The Occurrence, Prevention and Treatment of Sulfate. *Society of Petroleum Engineers*.

Chandler_Engineering. (2017, April 10). *Quizix QX Series*. Retrieved from ChandlerEngineering:

http://www.chandlerengineering.com/Products/Quizix%20Precision%20Pumps/QXSeries.aspx

Charleston, J. (1968). Scale Removal in the Virden, Manitoba, Area. *43rd Annual Fall Meeting of SPE of AIME* . Houston.

Chen, P., Vikane, O., & Asheim, T. (2006). ield Experiences in the Application of an Inhibitor/Additive Interaction Package to Extend an Inhibitor Squeeze Life. *Society of Petroleum Engineers*.

Dixon, M., & BiolinScientific. (2014). QCM-D Basic Training: Introduction and Applications. Gothenburg, Sweden.

Fink, J. (2003). *Oil Field Chemicals.* Gulf Professional Publishing.

Frenier, W., & Ziauddin, M. (2008). Formation, removal and inhibition of Inorganic Scale in the Oilfield Environment. *Society of Petroleum Engineers*.

Hsu, J., Al-Zain, A., & Raju., K. (2000). Encapsulated Scale Inhibitor Treatments experience in the Ghawar Field, Saudi Arabia. *Society of Petroleum Engineers*.

Huddersman, K. (2012). *Zeolites and Catalysis: Synthesis, Reactions and Applications.* Wiley–VCH.

Ibrahim, J., Sorbie, K., & Boak, L. (2012). Coupled Adsorption/Precipitation Experiments: 2. Non-Equilibrium Sand Pack Treatments. *SPE International Conference on Oilfield Scale.* Society of Petroleum Engineers.

Jurgawczynski, M. (2007, February). Predicting Absolute and Relative Permeabilities of Carbonate Rocks Using Image Analysis and Effective Medium Theory. *Thesis for PhD in the University of London*. Kensington, London, United Kingdom: Imperial College London.

Kelland, M. (2009). Production Chemicals for the Oil and Gas Industry. *CRC Press*.

Li, H.-Y., Ma, W., Wang, L., Liu, R., Wei, L.-S., & Wang, Q. (2006). Inhibition of calcium and magnesium-containing scale by a new antiscalant polymer in laboratory tests and a field trial. *Desalination 196*, 237-247.

Mackey, E. (2007). SPE Distinguished Lecture Series 2007-2008. SPE.

Martins, J., Kelly, R., & Lane, R. (1992). Scale Inhibition of Hydraulic Fractures in Prudhoe Bay. *Society of Petroleum Engineers*.

Mazzoline, E., Bertrro, L., & Truefitt. (1990). Scale Prediction and Laboratory
 Evaluation of BaSO4 Scale Inhibitors for Seawater Flood in High Barium
 Environment. *Europec 90.* Hague.

mrqsense. (2009, November 13). *Q-Sense Quartz Crystal Microbalance with Dissipation
 (QCM-D) technology animation*. Retrieved from YouTube:
 https://www.youtube.com/watch?v=NyscQUWxGoE

Murali, D., & Aloulou, F. (2016, August 22). *Today in Energy*. Retrieved from U.S.
 Energy Information Administration:
 http://www.eia.gov/todayinenergy/detail.cfm?id=27612

Pedenaud, P., Goulay, C., Pottier, F., Garnier, O., & Gauthier, B. (2006). Silica-scale
 inhibition for steam generation. *SPE Production and Operations*.

Poynton, N., Tidswell, R., & Steele, J. (2000). Squeezing Aqueous Based Scale
 Inhibitors into a Water Sensitive Scale problems in production. *Society of
 Petroleum Engineers*.

Qingfeng, Y. (2006). Inhibition of CaC03 Scaling in Reverse Osmosis System by Zinc
 Ion. *Chinese Journal of Chemical Engineering*, 179-183.

Selle, O., Wat, R., & Vikane, O. (2003). A Way Beyond Scale Inhibitors – Extending
 Scale Inhibitor Squeeze Life Through Bridging. *Society of Petroleum Engineers*.

Shaughnessy, C., & Kelly, W. (1983). EDTA Removes Formation Damage at Prudhoe
 Bay. *Journal of Petroleum Engineering*, 1783-1791.

Shuler, P. (1994). Clay-Induced Permeability Damage from Injected Scale Inhibitor
 Solutions. *Society of Petroleum Engineers*.

Smith, C., Nolan, T., & Crenshaw, P. (1968). Removal and Inhibition of Calcium
 Sulphate Scale in Waterflood Project. *Journal of Petroleum Technology*, 12149-
 1256.

Teledyne. (2017, April 10). *500D Syringe Pump*. Retrieved from TeledyneIsco:
 http://www.teledyneisco.com/pumpproducts/Pages/500D.aspx

Tomson, M. B., Kan, A., & Fu, G. (2004). Inhibition Of Barite Scale In The Presence Of
 Hydrate Inhibitors. *Society of Petroleum Engineers*.

Vetter, O. (1976). Oilfield Scale - Can We Handle It? *Journal of Petroleum Technology*,
 1402-1408.

Yan, C., Kan, A., Want, W., Yan, F., Wang, L., & Tomson, M. (2013). Synthesis and
 Sorption Study of AlOOH Nanoparticle Cross-Linked Polylmeric Scale
 Inhibitors and Their Squeeze Performance in Porous Media. *Society of Petroleum
 Engineers*.

Yen, T. (2016, February 18). *Today in Energy*. Retrieved from U.S. Energy Information
 Administration: http://www.eia.gov/todayinenergy/detail.cfm?id=25012

Yuan, M., Sorbie, K., & Todd, A. (1993). The Modelling of Adsorption and
 Precipitation Scale Inhibitor Squeeze Treatments in North Sea Fields. *Society of
 Petroleum Engineers*.

Zhang, Y., Wu, J., Hao, S., & Liu, M. (2007). Synthesis and Inhibition Efficiency of a
 Novel Quadripolymer Inhibitor. *Chinese Journal of Chemical Engineering*, 600-
 605.